CHAPTER IV

RESULTS & DISCUSSION

4. RESULTS AND DISCUSSION

4.1. INTRODUCTION :

One of the goals of materials research is to create new materials with physical properties tailored to a particular application and to understand the physical mechanisms which determine their properties.

The electrical conductivity of rubber composites attracts the attention of many authors[6, 30, 81]. The carbon black is still the most common conducting filler used. In carbon black loaded rubber composites it was found that the temperature coefficient of conductivity (TCC) is markedly affected by both *type and concentration* of carbon black[61,82]. For a given type of black the TCC of corresponding rubber composite *alters* its sign from *positive to negative* as the concentration of black *increases*. As a rule, the conductive rubber composites having negative TCC values can be used as heating elements.

It is well known that the addition of the ceramic materials to rubber composites *improves* their thermal

stability[3]. In section 4.2 , the effect of added $BaTiO_3$ on the electrical and thermal properties of conductive rubber were studied aiming to obtain heating elements based on rubber composites. In section 4.3, the effect of concentration of different types of carbon black on the electrical and thermal properties were discussed. To point out the *best conditions* at which these heating elements can operate, the influence of *some factors* such as the ambient temperature, ageing time and the sample dimensions were studied in section 4.4. Moreover, results on ac measurements were also carried out.

4.2. Effect of $BaTiO_3$ on the Electrical and Thermal Effects of Carbon Black-Loaded Butyl Rubber[83]:

In order to show the effect of barium titanate [$BaTiO_3$] - ceramics on the electrical conductivity of the conductive butyl rubber composites, different *concentrations* of $BaTiO_3$ powder were introduced into the butyl rubber containing 50 phr of LAMP black. Such concentration represents the *percolation* concentration of LAMP black at which maximum change in the electrical conductivity, σ, of the composite occurred[6]. This

means that the addition of small amount of any ingredients affecting the electrical conductivity can be markedly detected.

The results of this preliminary experiment are shown in Table 4.1.

Table 4.1: Effect of $BaTiO_3$ on the electrical conductivity of 50 phr LAMP black-loaded butyl rubber composites:

$BaTiO_3$ (phr)	0	10	20	30	40	50
σ, $(\Omega^{-1}cm^{-1})$	1.0×10^{-7}	5.6×10^{-7}	5.0×10^{-6}	6.0×10^{-8}	3.0×10^{-8}	1.0×10^{-8}

It is noticed from this table that, there is a marked increase in σ upon addition of $BaTiO_3$ up to 20 phr. Thereafter, σ decreases with increasing ceramic concentration. This behaviour could be explained as follows :

i) The first addition of $BaTiO_3$-ceramic starts to fill partially the free volume inside the rubber matrix forming ordered and/or crystalline phase. Added carbon black, in this

case should occupy the rest of free volume forming conducting pathways which, in turn, markedly increase the electric conduction. This phonomena was observed also by some authors using a blend of rubber and crystalline thermoplastic, namely, polyethylene[84].

ii) Upon further increase in $BaTiO_3$ concentration, the dilution effect of carbon black takes place resulting in a monotonic decrease in the electrical conductivity of such composites.

Taking into consideration the obtained results of this preliminary experiment, further study on the effect of $BaTiO_3$ on the electrical and thermal performances of the investigated samples is considered. For obtaining heating elements based on rubber composites, the electrical measurements of more conducting samples containing higher concentrations of carbon black [100 phr] have been performed.

One of the safty conditions to operate a heating element, is the limitation of the heating current passing through the sample upon increasing its temperature due to Joule heating effect. The results obtained on investigated conductive rubber

composites presented in the following sections satisfy this condition.

4.2.1. Temperature dependence of the electrical conductivity:

Figure **4.1** illustrates the temperature dependence of the electrical conductivity of 100 phr black-loaded butyl rubber. It is noticed that most of the samples show negative values of the temperature coefficient of conductivity [TCC] over the temperature range used.

This descending behaviour of the electrical conductivity with temperature could be explained as follows :
Let us consider the carbon black particles or aggregates as spheres embedded into the rubber matrix at an average separation distances of insulating rubber material. These insulating separation distances play an important role in the conduction mechanism. At relatively small value of the separation distance, tunnelling conduction is most propable[85]. Taking into account the high value of the thermal expansion coefficient of rubber [$\cong 200 \times 10^{-6}$ deg^{-1}][86] with respect to that of carbon black [$\cong 1.0 \times 10^{-6}$ deg^{-1}],[87] the decrease in

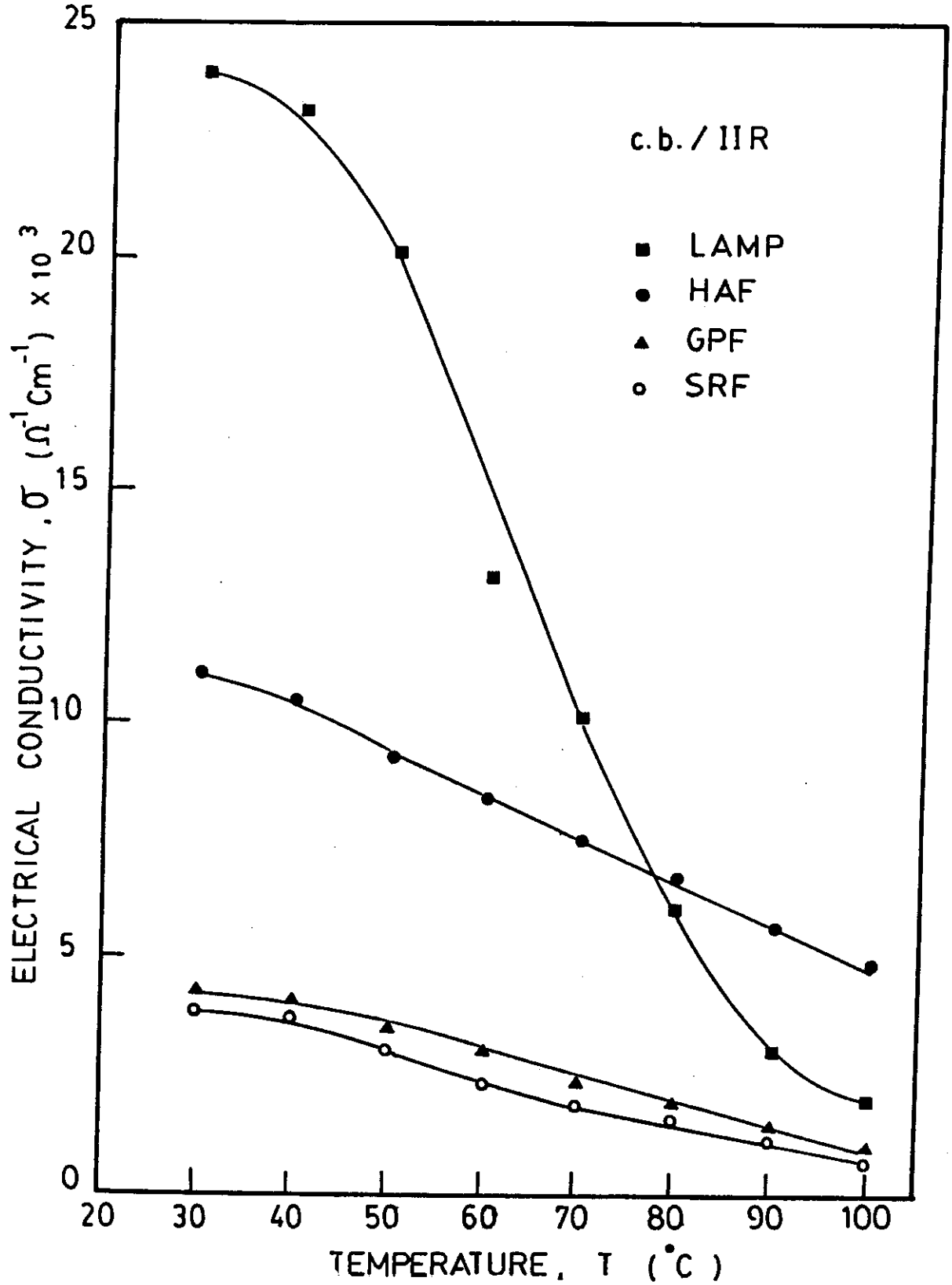

Fig. [4.1] : The temperature dependence of the electrical conductivity for carbon black-loaded butyl rubber.

σ with temperature is due to the thermal expansion of the tunnelling paths between the conducting carbon particles or aggregates.

One of the important parameters governing the variation of the electrical conductivity, σ, with temperature, T, is the temperature coefficient of conductivity [TCC] where:

$$TCC = \delta\sigma / \sigma \delta T \qquad (4.1)$$

The addition of 20 phr of $BaTiO_3$ affects both the electrical conductivity and TCC of the above conductive composites as shown in figure 4.2. Generally speaking, the addition of 20 phr $BaTiO_3$ increases the electrical conductivity and also decreases the values of TCC which even approaches zero value for GPF and SRF filled composites. Increasing the carbon black concentration up to 100 phr enhances the formation of stable conducting pathways of carbon black particles or aggregates. Consequently, detectable increase in the electrical conductivity occurs. In addition, the nearly temperature independent behaviour of the electrical conductivity of some types of carbon black, could

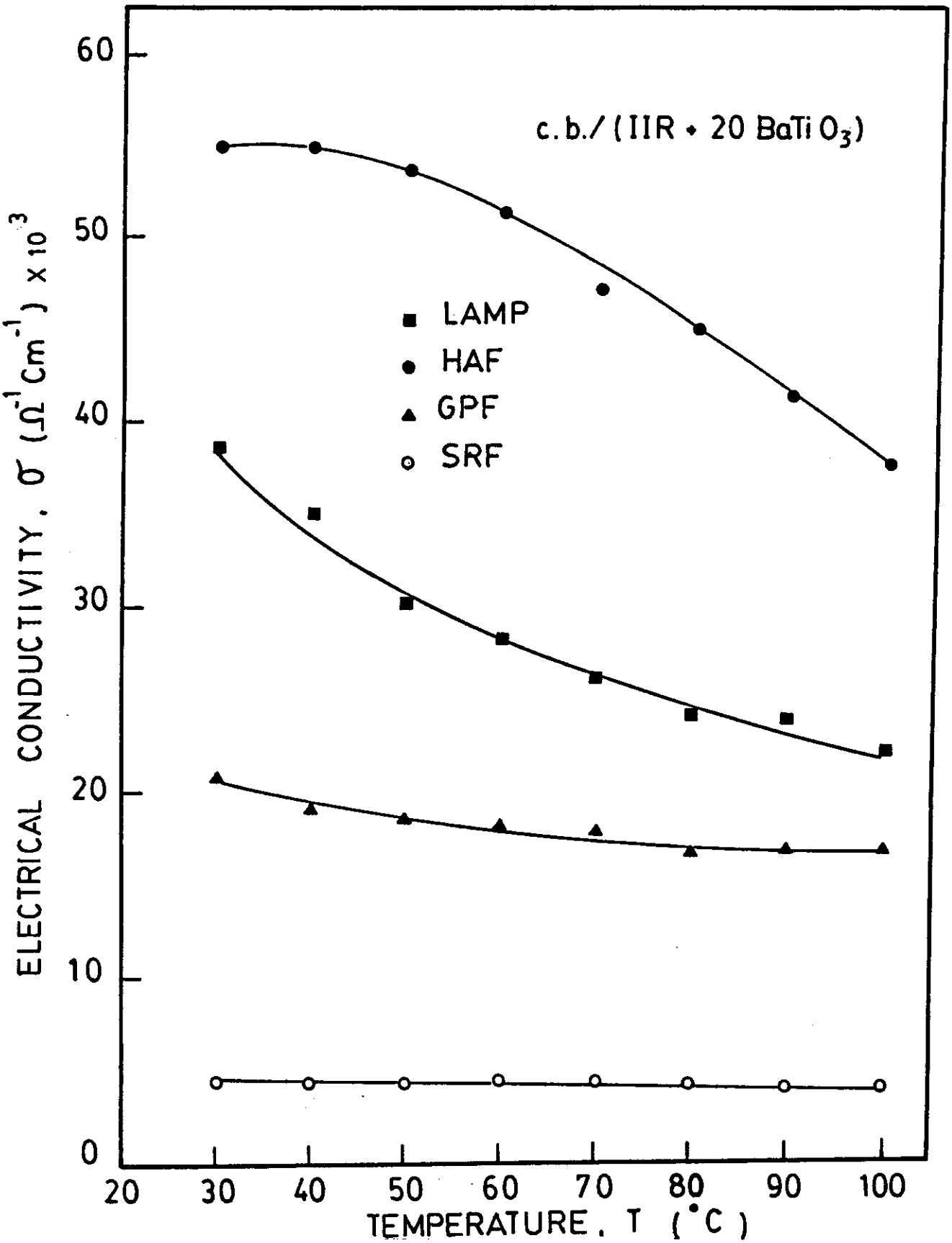

Fig. [4.2] : The temperature dependence of the electrical conductivity for carbon black-loaded butyl rubber containing 20 phr $BaTiO_3$.

be explained as a result of competition of two conduction mechanisms. The first one is the decrease in the electrical conductivity upon the thermal expansion of the hopping and/or tunnelling paths and the second mechanism is the thermally activated electrical conductivity of the semiconducting black filler.

Table 4.2 illustrates the calculated values of $[TCC]_{max.}$ and the corresponding temperatures attained of this rubber composite.

The improvement obtained in both σ and TCC upon the addition of $BaTiO_3$, allaws us to carry out further study on the I–V–T characterisitic curves of the above composites.

4.2.2: Current-Voltage-Temperature Characteristics :

In order to use these conducting composites as heating elements, it is useful to follow up the variation in the sample temperature ,due to Joule heating, upon increasing the applied electric power. For this purpose, the Current – Voltage – Temperature [I-V-T] characteristics of such composites were evaluated.

Table 4.2: The calculated values of $[TCC]_{max.}$ for carbon black-loaded butyl rubber composites with and without $BaTiO_3$.

Sample	T (°C)	$[TCC]_{max.}$ (deg^{-1})
H10	50	0.012
G10	80	0.030
S10	80	0.040
L10	80	0.100
CH10	90	0.014
CG10	40	5.0×10^{-3}
CS10	35	5.5×10^{-4}
CL10	50	0.013

Figuer 4.3 illustrates the I–V–T curves for 100 phr black – loaded butyl rubber composites. The solid curves represent the I–V dependence, while the dashed ones represent the variation of the ultimate temperature [T_m] with the applied voltage. It was observed that for low values of electric power, the Ohmic behaviour is predomenant without any remarkable change of the sample temperature. Increasing the electric power above a certain limit [>0.1 watt/cm^3] leads to an increase in the Joule heating effect and consequently increase in the sample temperature. As a result a deviation of I–V characteristic from the Ohmic behaviour is observed. This sub–Ohmic behaviour obtained upon Joule heating could be understood by taking into consideration the negative value of the TCC of these composites [Cf. Table 4.2].

Figure 4.4 illustrates the reproduced data of the I–V–T characteristic for the above composites containing 20 phr $BaTiO_3$. It was noticed that the addition of barium titanate increases the ultimate temperature, produced by Joule heating for the same applied electric potential.

Figure 4.5 shows the variation of the electrical conductivity, σ, with the temperature produced by Joule

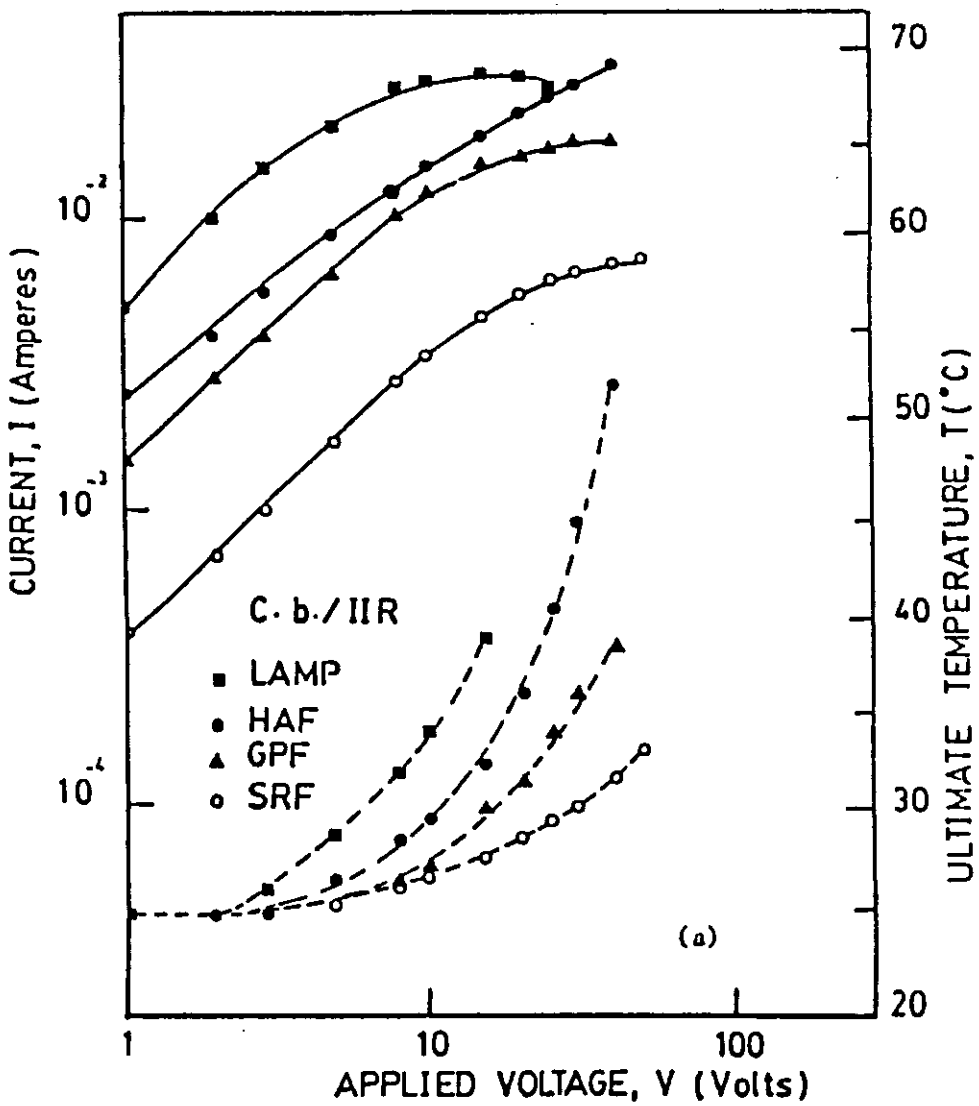

Fig. [4.3] : I-V-T curves for carbon black-loaded butyl rubber vulcanizates.

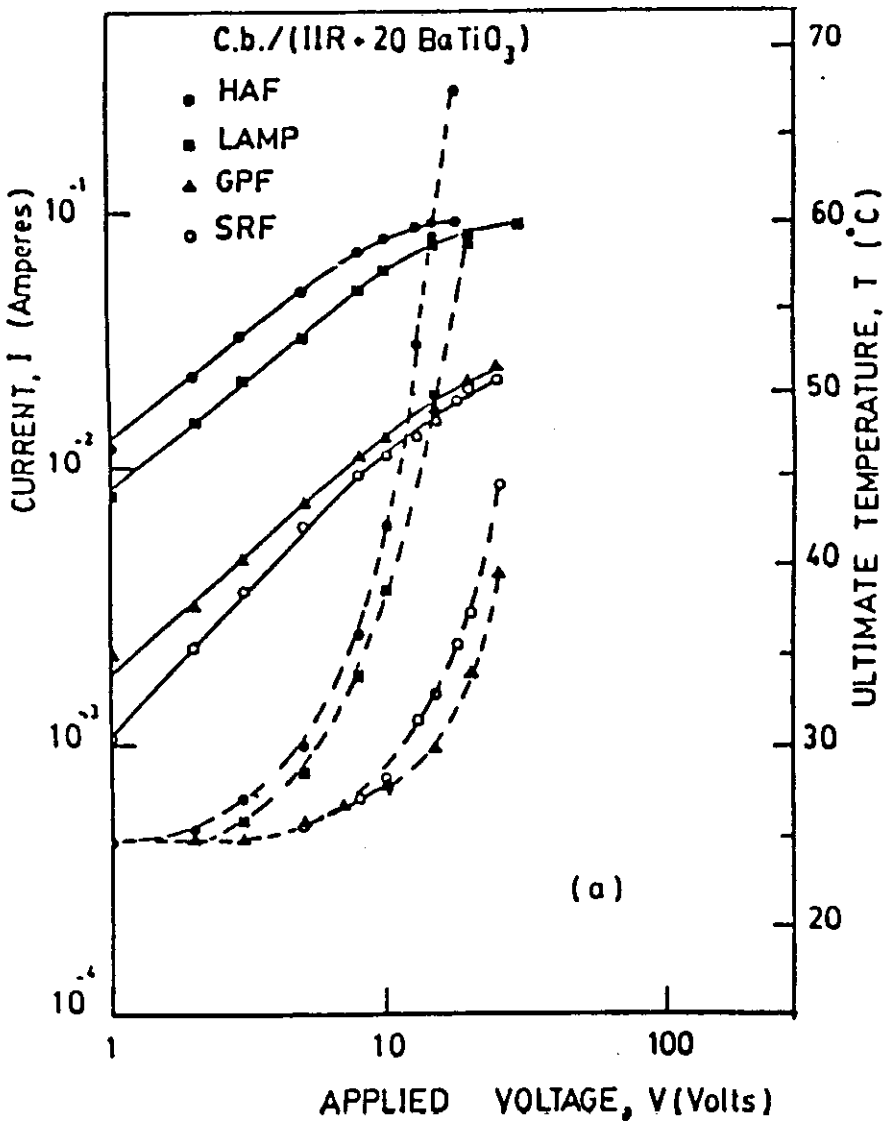

Fig. [4.4] : I-V-T curves for carbon black-loaded butyl rubber vulcanizates containing 20 phr $BaTiO_3$.

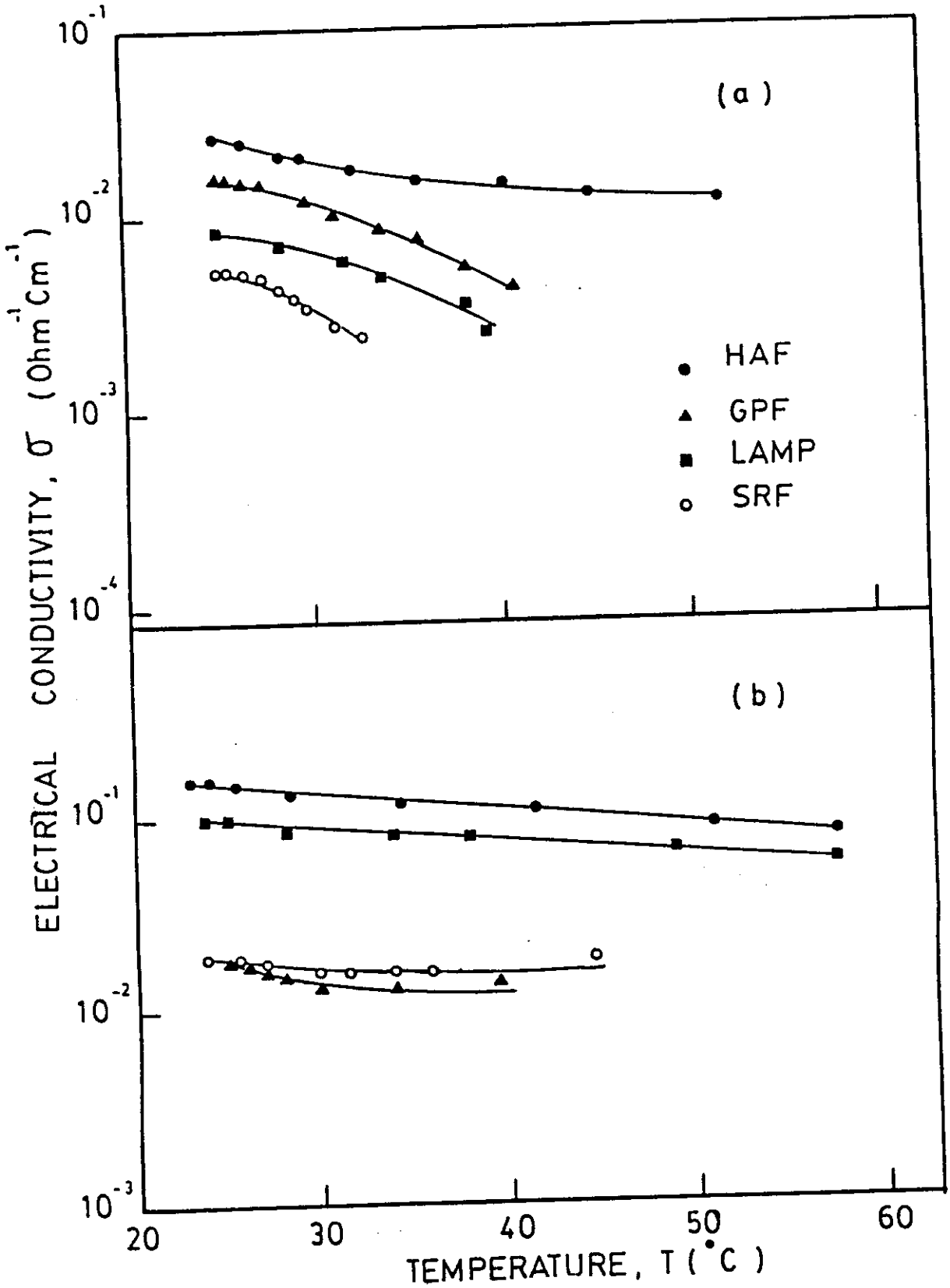

Fig. [4.5] : The variation of the electrical conductivity with temperature (produced by Joule effect) for carbon black-loaded butyl rubber composites. (a) without $BaTiO_3$ and (b) with 20 phr $BaTiO_3$.

heating and deduced from the previous figuers. The decrease in σ with temperature confirms the thermal expansion of the hopping and/or tunnelling paths between either carbon-carbon particles or aggregates. The increase in temperature may be either *externally* [Figs. 4.1 and 4.2] or *internally* due to Joule heating, [Fig. 4.5].

Table 4.3 summerizes the calculated values of the $[TCC]_{max.}$ obtained from figure 4.5. These data are in a good agreement with that obtained previously in section 4.2 for the role of the addition of $BaTiO_3$.

Figure 4.6 illustrates the dependence of the ultimate temperature, T_m, of the sample on the applied electric power, P, deduced from the above data. The T_m – P dependence can be represented by the following empirical formula :

$$T_m = a\,[P/P_o]^b + T_o \qquad (4.2)$$

where T_o is the room temperature, a and b are fitting parameters, and P_o is a reference power taken as unity.

Equation 4.2 represents a straight line relationship

Table 4.3: The calculated values of $[TCC]_{max}$ from Fig. 4.5.

Sample	T (°C)	$[TCC]_{max.}$ (deg^{-1})
H10	28	0.060
G10	35	0.110
S10	32	0.140
L10	36	0.115
CH10	42	0.021
CG10	28	0.050
CS10	25	0.021
CL10	35	0.016

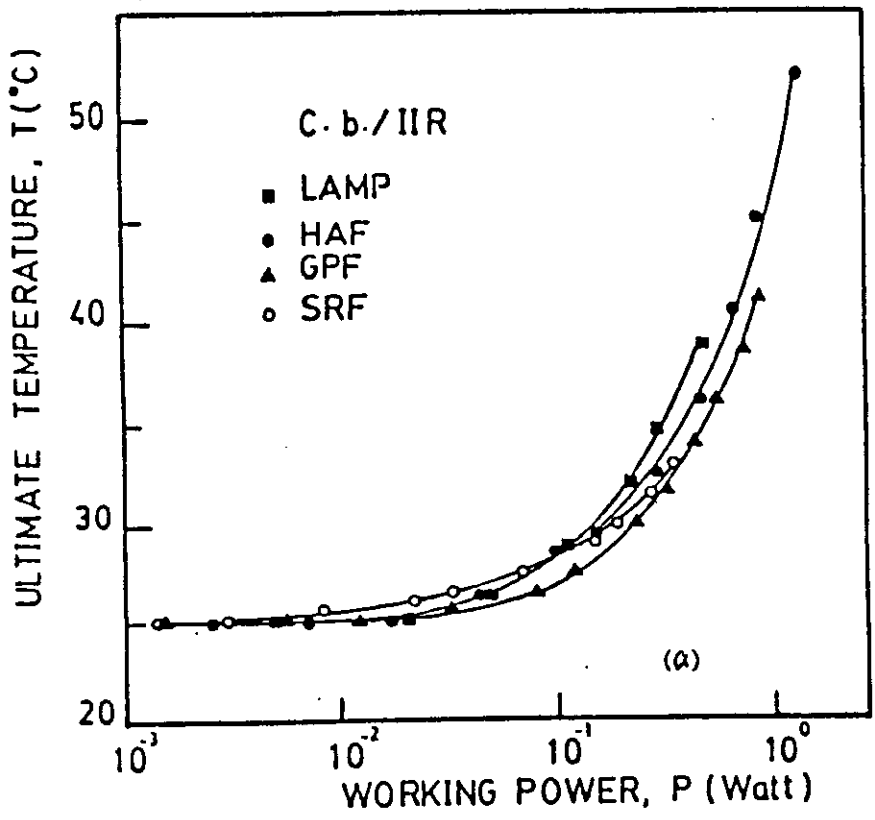

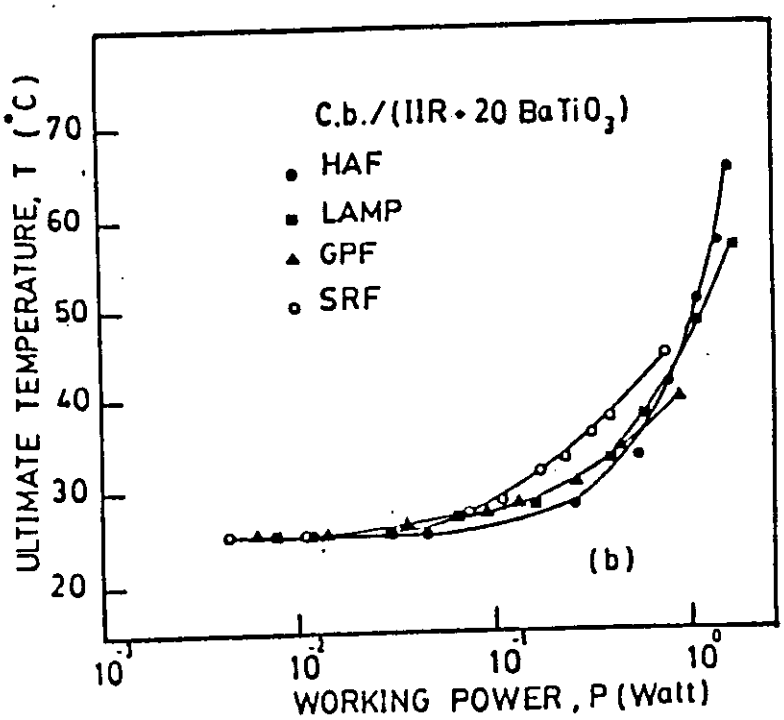

Fig. [4.6] : T-P curves for carbon black-loaded butyl rubber vulcanizates. (a) without $BaTiO_3$ and (b) with 20 phr $BaTiO_3$.

between $[T_m - T_o]$ and P on the log-log scale [not mentioned here] with slope equals b and intersection equals log a. The parameter a represents the difference in temperature produced by Joule heating when $P = P_o = 1$ watt.

Table 4.4 summerizes the calculated values of the fitting parameters a and b for the investigated rubber composites. From this table it is shown that the addition of barium titanate increases, in general, the temperature difference produced by Joule effect per watt.

4.2.3 : Temperature-time Characteristics :

In order to calculate some useful thermal parameters such as the *specific heat* and the *amount of heat transfered by radiation and convection*, the surface temperature of the rubber samples was recorded as a function of time during the heating and equilibrium temperature. In addition the cooling curve, after the cut-off of the electric power, was also obtained.

Figure 4.7 presents the temperature-time [T-t] characteristics of the above composites at initial value of the electric

Table 4.4 : The calculated values of the fitting parameters, a and b.

Sample	a (deg)	b
H10	22.4	0.85
G10	19.0	0.93
S10	15.1	0.68
L10	23.5	0.90
CH10	26.0	1.14
CG10	18.0	0.85
CS10	31.6	1.00
CL10	25.5	0.97

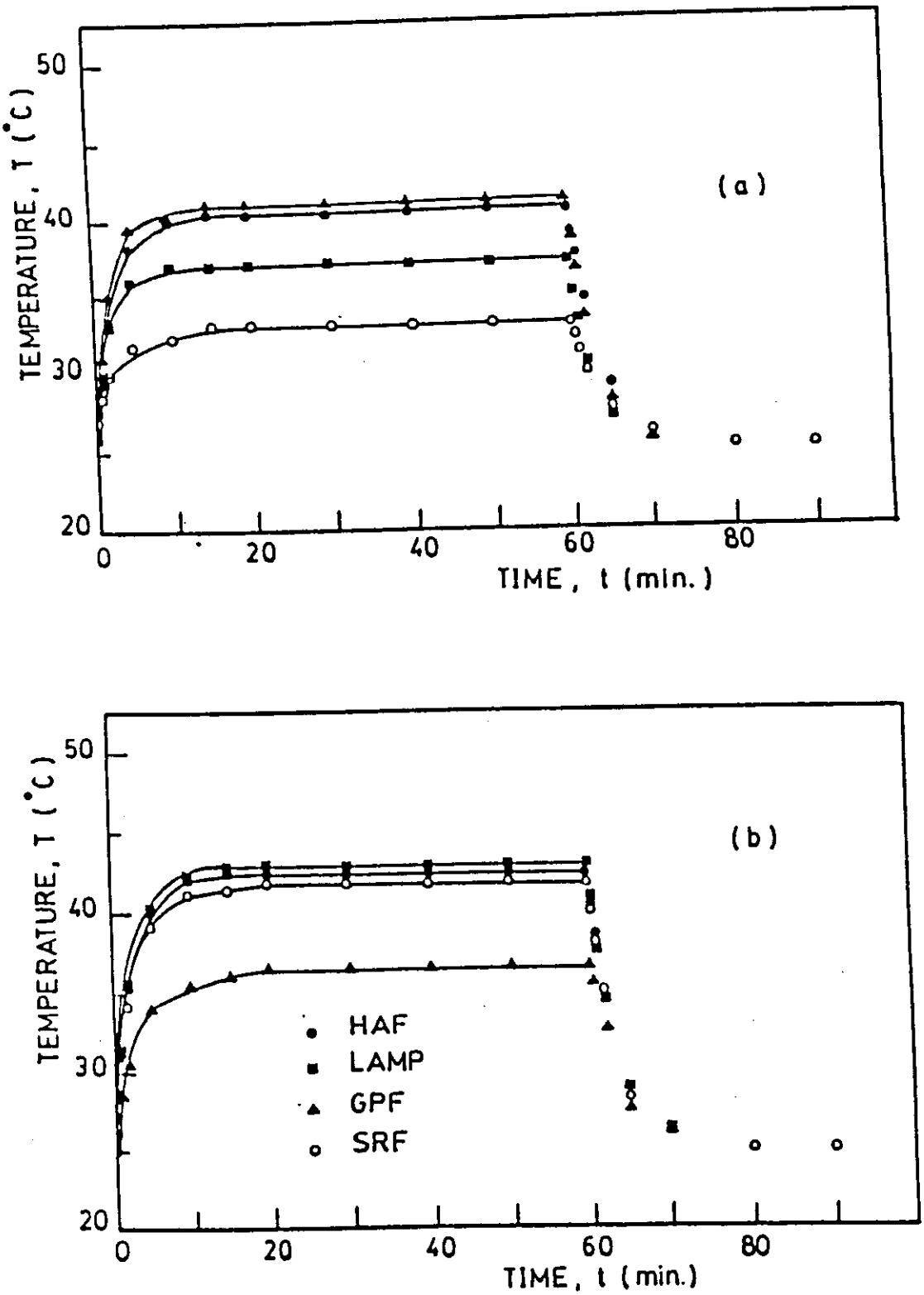

Fig. [4.7] : The temperature-time characteristics for carbon black-loaded butyl rubber vulcanizates. (a) without $BaTiO_3$ and (b) with 20 phr $BaTiO_3$.

power equals 1 watt. After attaining equilibrium temperature the power was cut-off and the temperature decay was recorded with time. It is obvious, again, that the ultimate temperature value per watt depends on the type of carbon black used as well as the presence of $BaTiO_3$. [Cf. Table 4.4].

The curves showing the temperature - time [T-t] characteristics for all investigated composites can be divided into three regions, namely ;

i) the temperature growth [heating] region,
ii) the equilibrium [ultimate] temperature region, and
iii) the temperature decay [cooling] region.

Figure 4.8 illustrates the general feature of these three regions [solid curve] in addition to the variation of the conduction current inside the test sample [dashed curve] for conductive rubber sample [100 LAMP/(IIR + 20 $BaTiO_3$)].

In region I, the temperature growth with time for an initial power $I_o V_o$ can be represented by an exponential growth function as :

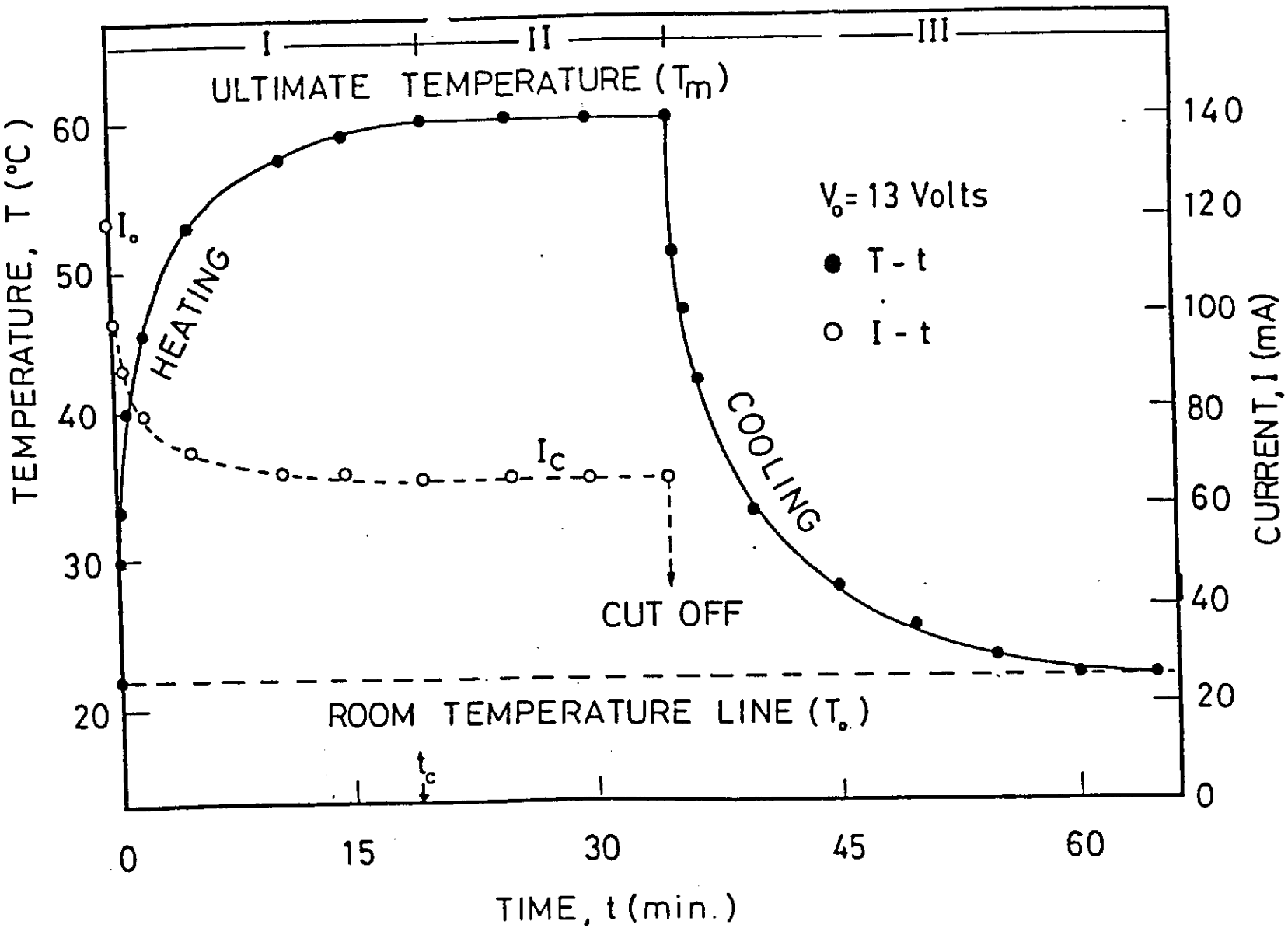

Fig. [4.8] : The T(t) and I(t) curves for carbon black-loaded butyl rubber vulcanizate.

$$T(t) - T_o = (T_m - T_o)\,[\,1 - \exp(-t/\tau_g)\,] \qquad (4.3)$$

where T_o and T_m are the ambient and the ultimate temperatures respectivily, and τ_g is the time constant depending on the type of carbon black as well as the addition of $BaTiO_3$ ceramics [Cf. Table 4.5].

It was found, by *curve fitting*, that the conduction current varies with time as follows:

$$I(t) - I_c = (I_o - I_c)\,[\,\tau_i/(t + \tau_i)\,] \qquad (4.4)$$

where τ_i is the current time constant depending on the type of carbon black as well as the presence of $BaTiO_3$ ceramics [Cf. Table 4.5].

The conservation law of energy, in region I, requires that ;

$$I(t)\,V_o\,t_c = mC_p\,(T_m - T_o) + A\,(h_r + h_c)\,[T(t) - T_o] \qquad (4.5)$$

where t_c is the time at which the current reaches its steady

state value (I_c); C_p is the specific heat of the specimen; m its mass, h_r and h_c are the amount of heat transfer per unit area per degree per second by radiation and convection respectivily[88], and A is the area of the specimen in m^2. Substituting from equations 4.3 and 4.4 in equation 4.5 one obtain :

$$\int_0^{t_c} I(t)\, V_o dt = mC_p(T_m - T_o) + A(h_r + h_c)(T_m - T_o)\int_0^{t_c} [1 - \exp(-t/\tau_g)]dt \quad \ldots\ldots(4.6)$$

and,

$$C_p = [m(T_m - T_o)]^{-1}\left[V_o(I_o - I_c)\tau_i \ln[(t_c+\tau_i)/\tau_i] + V_o I_c t_c - A(h_r + h_c)(T_m - T_o)\,[t_c - \tau_g\,[1-\exp(-t_c/\tau_g)]]\right] \quad \ldots\ldots(4.7)$$

From equation 4.7 *the specific heat* of the composites can be calculated from region I

Region II represents the equilibrium region and the conservation law of the energy can be written as follows :

$$I_c V_o = A (h_r + h_c) (T_m - T_o) \qquad (4.8)$$

In region III, during which the working power is switched off, the specimen is left to cool down by radiation and convection according to *Newton's* law of cooling. The temperature varies with time as follows :

$$T(t) - T_o = (T_m - T_o) \exp [-t/\tau_d] \qquad (4.9)$$

where τ_d is a time constant which depends also on the type of carbon black and on the addition of $BaTiO_3$ ceramics. [Cf. Table **4.5**].

The conservation law of energy, in region III, gives the following equation :

$$m C_p (T_m - T_o) = A (h_r + h_c) [T(t) - T_o] \qquad (4.10)$$

Substituting from equation **4.9** in equation **4.10** one obtains

$$mC_p(T_m - T_o) = A (h_r + h_c) (T_m - T_o) \int_0^{t_o} \exp [- t/\tau_d] \, dt \qquad (4.11)$$

where t_o is the time required for the temperature of the sample to attain T_o.

Thus, we get :

$$C_p = [1/m]\left[A (h_r + h_c) \tau_g [1 - \exp [- t_o/\tau_g]]\right] \qquad (4.12)$$

From which one can again calculate the *specific heat* of the composites from region III.

Table 4.5 illustrates the calculated values of the time constants τ_g, τ_i, and τ_d, the specific heat, Cp, [from region I and region III] , and the amount of heat transferred by radiation and convection, $[h_r + h_c]$, for the different types of carbon black . From this table it is shown that the calculated values of the specific heat are in good agreement with the published data obtained by *Wood* and *Bekkedahl*(89) during their calorimetric measurements on large number of polymeric materials.

In addition the calculated values of Cp obtained from the different regions, I and III, which are approximately

Table 4.5 : The calculated values of the time constants τ_g, τ_i, and τ_d, specific heat and the amount of heat transferred by radiation and convection. for the investigated rubber composites.

Sample	τ_g (min)	τ_i (min)	τ_d (min)	C_{p_I} [J/gm.deg]	$C_{p_{III}}$ [J/gm.deg]	$(h_r + h_c)$ [J/m^{2}deg.sec]
H10	2.50	0.4	3.60	3.04	3.97	36.2
G10	2.44	0.30	2.95	3.03	2.94	28.1
S10	3.00	0.16	3.50	5.00	6.40	38.7
L10	2.00	0.32	2.80	4.12	4.21	39.5
CH10	2.17	0.67	2.70	3.95	2.75	36.4
CG10	3.33	0.37	3.85	4.17	5.18	55.6
CS10	2.70	0.27	2.70	4.14	3.37	44.1
CL10	3.00	0.14	2.85	3.25	2.65	28.4

the same which confirm the mathematical treatement suggested for the [T-t] characteristics. From the calculated values of the amount of heat transfer per unit sample area per degree per second ($h_r + h_c$), one can determines the optimum working conditions to warm a given volume at a given initial boundary conditions[90].

In order to find the optimum concentration for each type of carbon black yeilds the maximum amount of energy transfer, different concentrations from each type of carbon black were introduced into rubber matrix.

4.2.4 : Thermal Conductivity :

The thermal properties of polymers are observed when thermal energy (*heat*) is added to or removed from a material. These properties include thermal conductivity and thermal diffusivity which is the ability to move heat (i.e. the rate of heat transfer by conduction).

In order to confirm the results obtained before, an alternative method was used for measuring specific heat, C_p and also the thermal conductivity, λ and thermal diffusivity, δ. This method was generally called "*flash method*", in which one surface of the sample was irradiated by a heating pulse for a short time and the temperature is monitored on the rear face of the sample (Cf. sec. 3.4).

As shown by *Parker et al.*[91], the temperature history of the rear face of a sample of length L is given by:

$$T(L,t) = \left[\phi / \rho C_p L \right] \left[1 + 2 \sum_{n=1}^{\infty} (-1)^n \exp \left[-(n^2 \pi^2 \delta t)/L^2 \right] \right], \ldots \quad \ldots\ldots(4.13)$$

where ϕ is the heat energy per unit area falling on the front surface and ρ is the sample density. This can be expressed in dimensionless form as a fraction of the maximum temperature T_{max} of the rear surface:

$$T(T,t)/T_{max}(T,t) = 1 + 2 \sum_{n=1}^{\infty} (-1)^n \exp \left[-(n^2 \pi^2 \delta t)/L^2 \right], \ldots \quad \ldots\ldots(4.14)$$

The graphical representation of eq. 4.14 is shown in figure 4.9.

As long as heat losses are negligible, the tangent to the temperature–time curve at the point of maximum gradient can be extrapolated to the time axis where the intercept, as shown in figure 4.9, occure at $\pi^2 \delta t / L^2 = 0.48$ from which

$$\delta = (0.48\ L^2)/(\pi^2\ t_x) \quad \ldots\ldots(4.15)$$

where t_x is the time axis intercept of the measured temperature–time curve.

If the energy absorbed by the front face is known, then

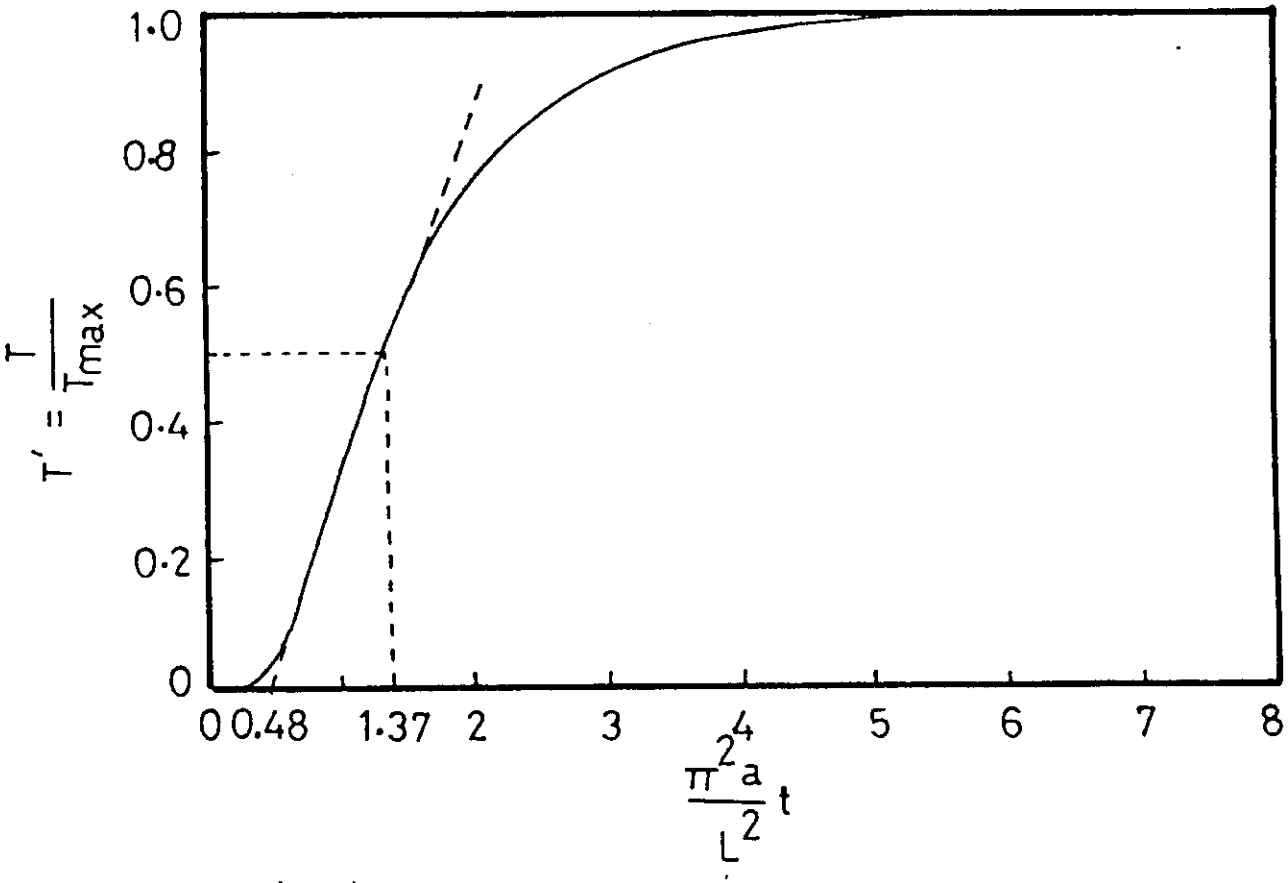

Fig. [4.9] : The rear face temperature gradient.

the specific heat of the sample is given by

$$C_p = \phi / (\rho L T_{max}) \qquad .....(4.16)$$

and the thermal conductivity (λ) can be evaluated from the following relation:

$$\lambda = \rho C_p \delta \qquad .....(4.17)$$

Also by knowing the information about a standared sample (weight, dimensions and Cp), we can find out the specific heat of the sample under investigation accordin to the relation :

$$[M_1 C_{p_1} (dT_1/dt_1)] / A_1 = [M_2 C_{p_2} (dT_2/dt_2)] / A_2 \qquad (4.18)$$

then,

$$C_p \text{ (sample)} = \left[[M_2 C_{p_2} (dT_2/dt_2)] / A_2 \right] * \left[A_1 / [M_1 (dT_1/dt_1)] \right] \qquad .....(4.19)$$

where, M_1, C_{p_1}, dT_1/dt_1 and A are the mass, specific heat, temperature gradient and area of the sample under investigation respectivily. M_2 ,C_{p_2} ,dT_2/dt_2 and A are the mass, specific heat, temperature gradient and area of the standered Cu sample.

Figure **4.10** illustrates the general feature of the temperature-time curve for an investigated sample, using the flash method technique, taken as an example to illustrates

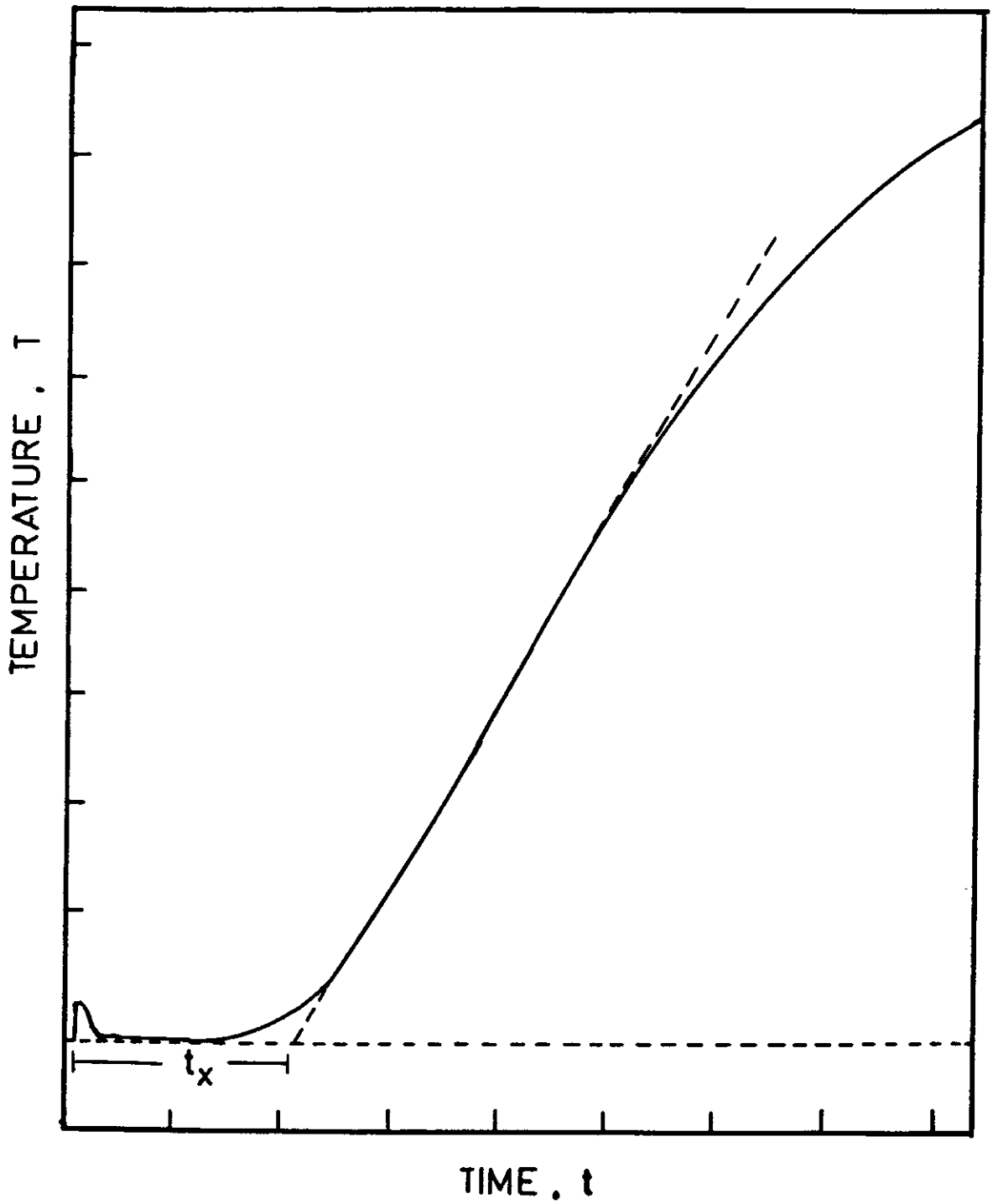

Fig. [4.10] : The temperature-time curve for an investigated carbon black-loaded butyl rubber composite.

the temperature response of the rear face of the sample.

Table 4.6 summerizes the calculated values of the thermal conductivity, thermal diffusivity and specific heat for the samples without and with 20 phr $BaTiO_3$. From this table its noticed that the addtion of $BaTiO_3$ rises, in general, the values of thermal conductivity. This may be attributed to the higher values of the heat capacity of ceramic materials. These data are in good agreement with that obtained by *Hands and Hosfatt*[92] for some polymeric materials.

Table 4.6: The calculated values of the thermal conductvity λ, thermal diffusivity δ, and specific heat C_p for the investigated rubber composites.

Sample	λ [Watt/m deg.]	δ [cm^2/sec.]	C_p [J/gm.deg.]
H10	0.597	1.5×10^{-3}	3.201
G10	0.401	1.4×10^{-3}	2.311
S10	0.486	1.5×10^{-3}	2.632
L10	0.429	1.5×10^{-3}	2.326
CH10	0.725	1.3×10^{-3}	4.00
CG10	0.437	1.1×10^{-3}	2.321
CS10	0.728	1.4×10^{-3}	3.960
CL10	0.540	1.5×10^{-3}	2.734

4.3 : Effect of Carbon Black Concentration on the Electrical and Thermal Effects of Carbon Black-Loaded Butyl Rubber :

In the present section, the effect of carbon black concentration on the electrical properties and the thermal parameters of $BaTiO_3$-loaded butyl rubber composites was studied. Different concentrations of four types of carbon black **HAF, GPF, SRF, and LAMP** black were introduced in the rubber matrix. These four types differ from each other by their surface area, particle size, and consequently other physical properties.
Accordingly, different characteristics either electrical or thermal for the same concentration can be expected.

Figure **4.11** illustrate the temperature dependence of the electrical conductivity of [IIR + 20 $BaTiO_3$] composites loaded with different concentrations of carbon black ; **a) GPF, b) HAF, c) LAMP, d) SRF.**

It is noticed, in general, that most of the investigated samples posses a negative values of the temperature

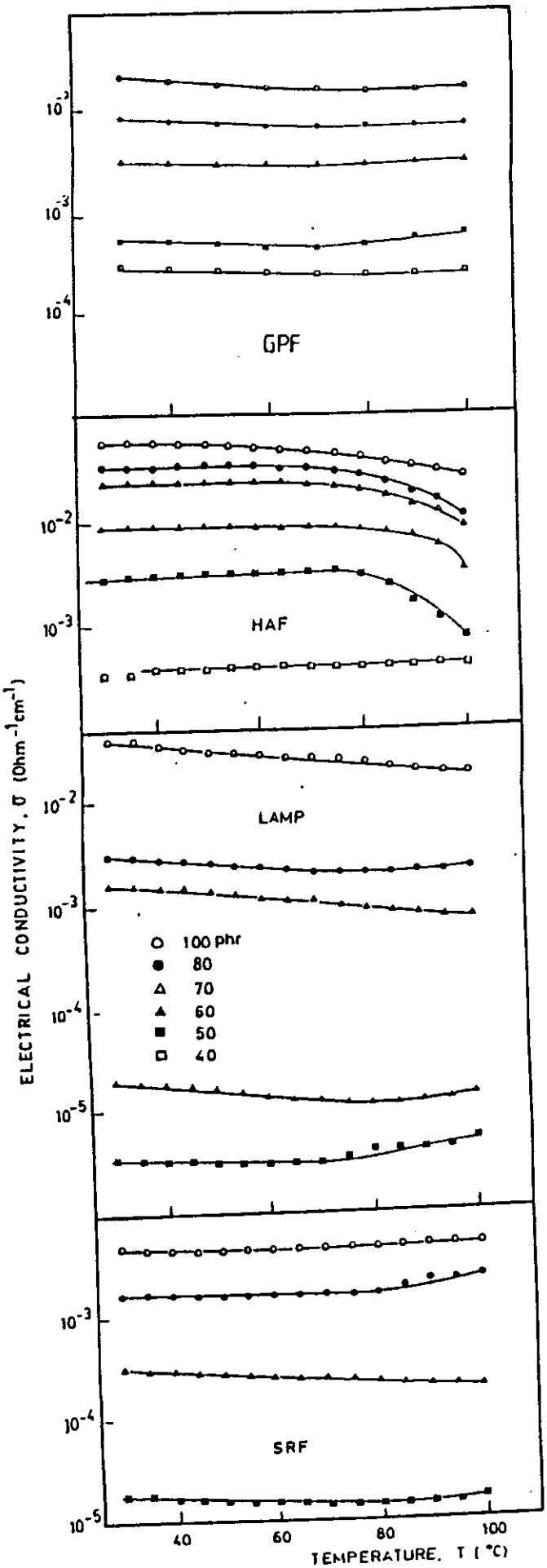

Fig. [4.11]:

The temperature dependence of the electrical conductivity of butyl rubber composites loaded with different concentrations of carbon black.

coefficient of conductivity [TCC] for the temperature range used.

The results illustrated in figures 4.12 - 4.15 summerize the Current-Voltage-Temperature [I-V-T] characterisitic curves as well as the dependence of the ultimate temperature [T_m] on the working power [P] for the above rubber composites. It is noticed from these figures that the I - V characteristic curves deviate from the Ohmic behaviour in case of HAF more than in case of GPF or SRF. This deviation being very large in case of LAMP black.

Each point on the Current-Voltage-Temperature [I-V-T] characteristic curves was obtained by recording the ultimate temperature attained after the power onset for sufficiently long time. Figures 4.16 - 4.19 present the temperature-time characteristic curves of the above composites. After equilibrium the power was cut off and the temperature decay was recorded with time. It is obvious from these figures that the value of the ultimate temperature per watt depends on the type and concentration of carbon black.

Table 4.6 illustrates the calculated values of the

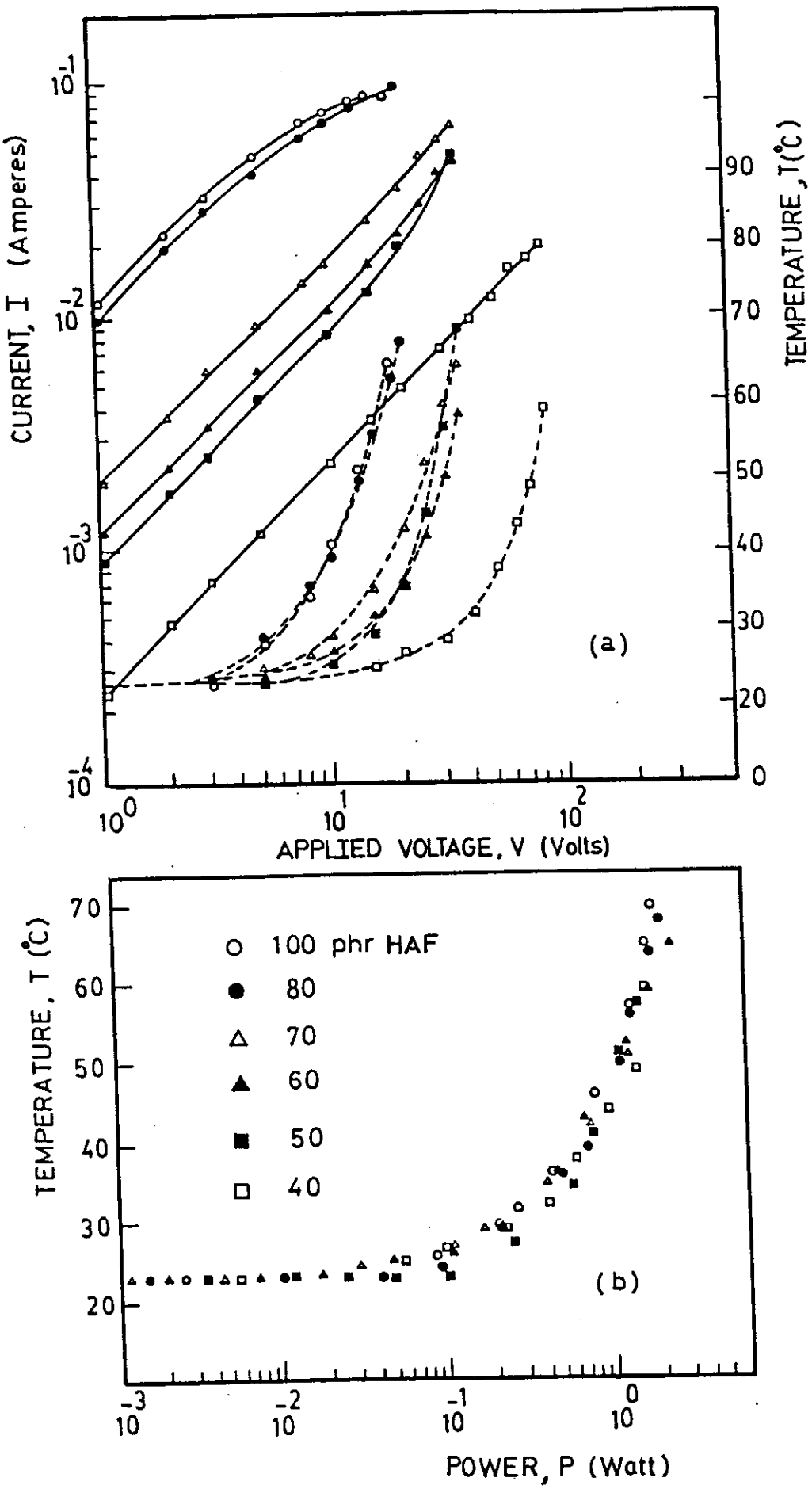

Fig. [4.12] : I-V-T and T-P curves for HAF black-loaded butyl rubber composites.

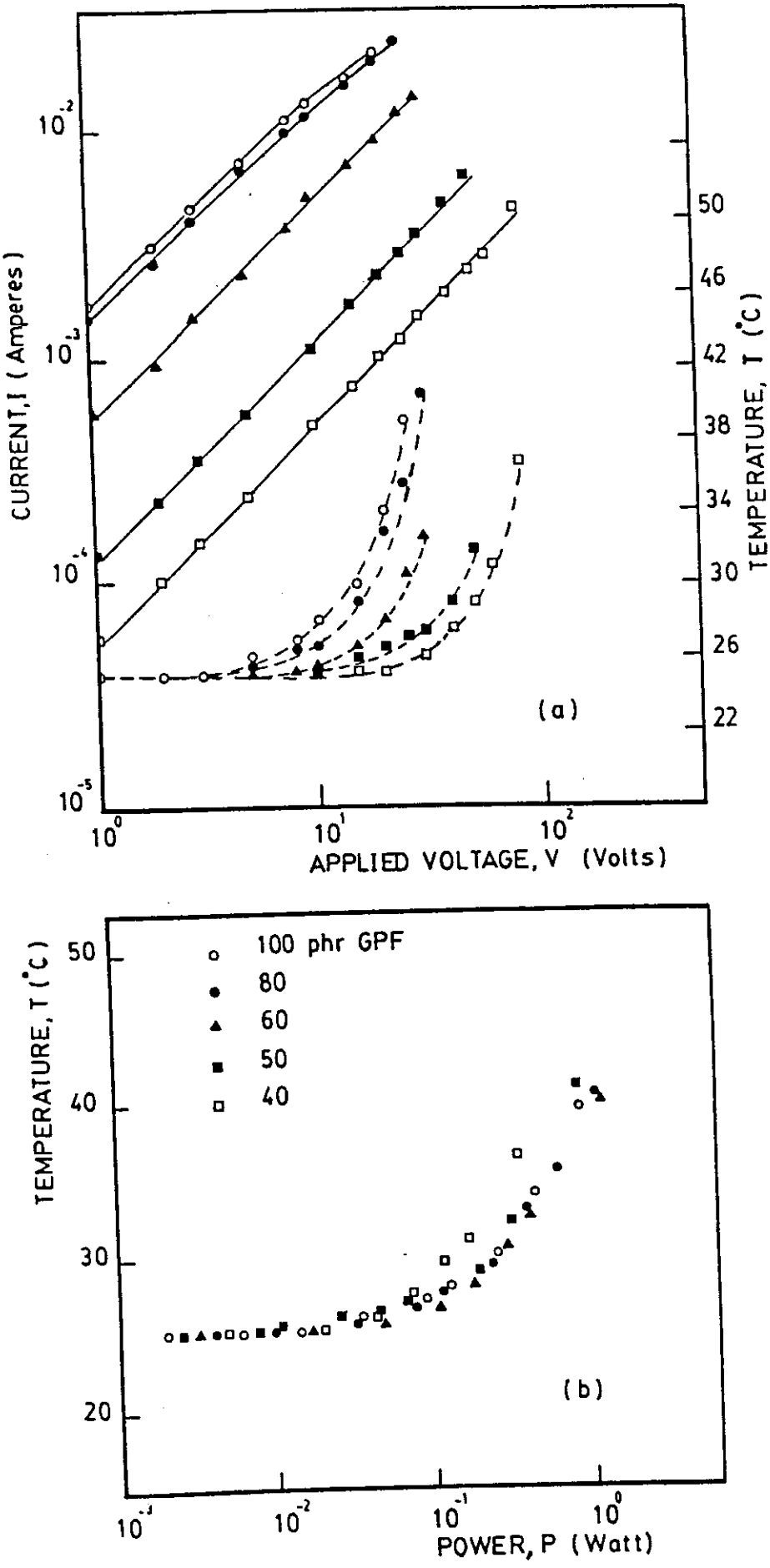

Fig. [4.13] : I-V-T and T-P curves for GPF black-loaded butyl rubber composites.

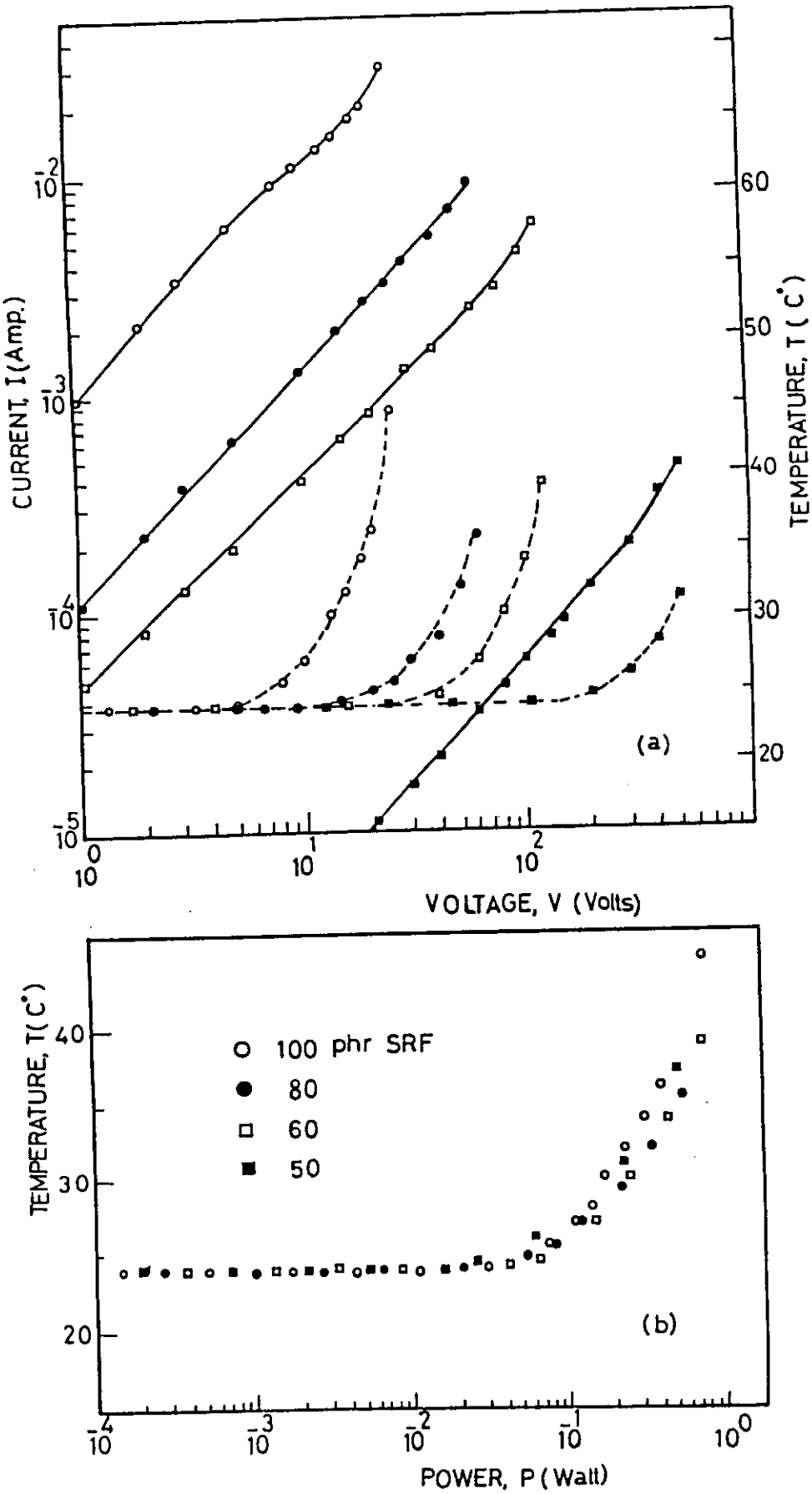

Fig. [4.14] : I-V-T and T-P curves for SRF black-loaded butyl rubber composites.

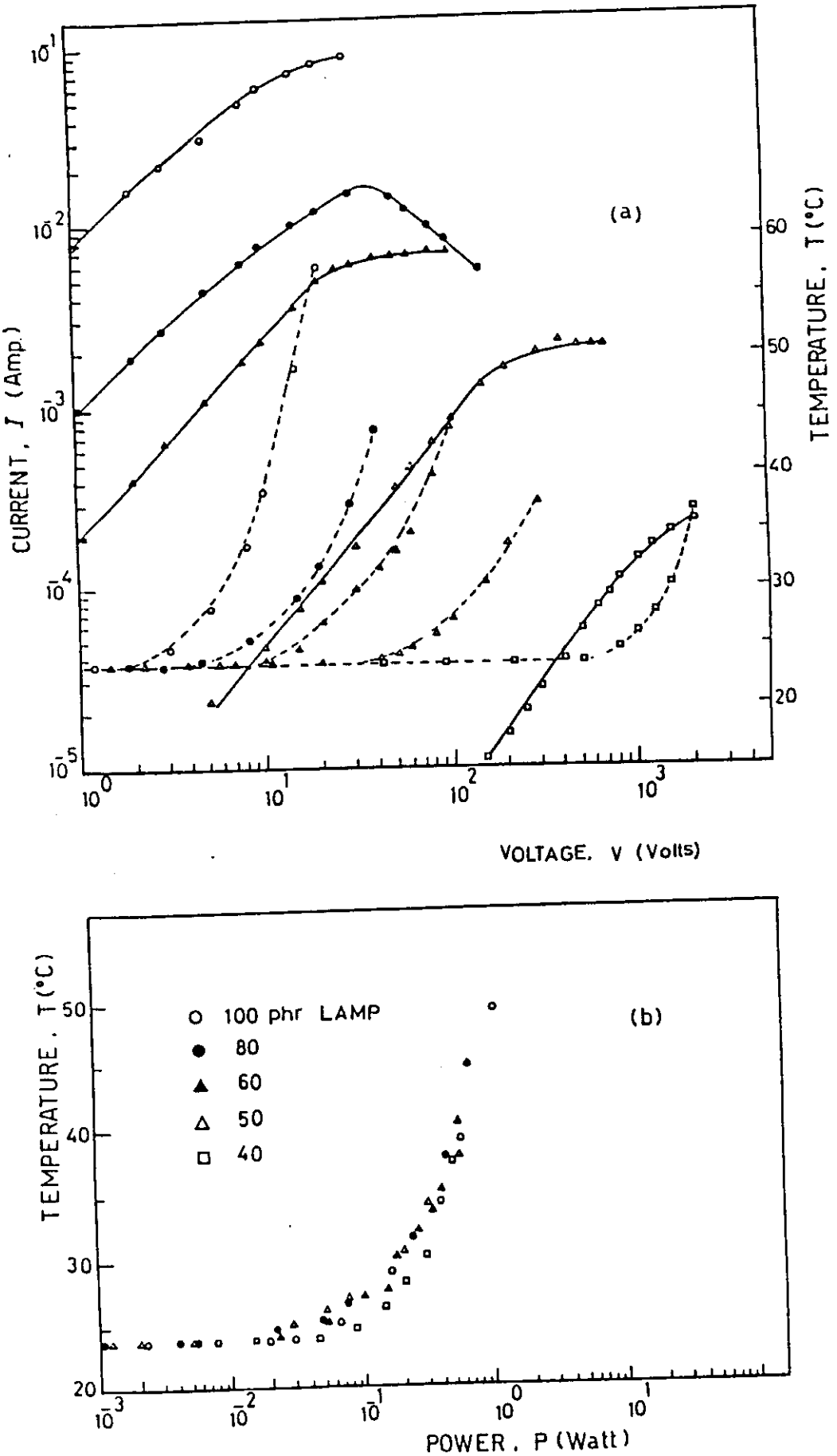

Fig. [4.15] : I-V-T and T-P curves for LAMP black-loaded butyl rubber composites.

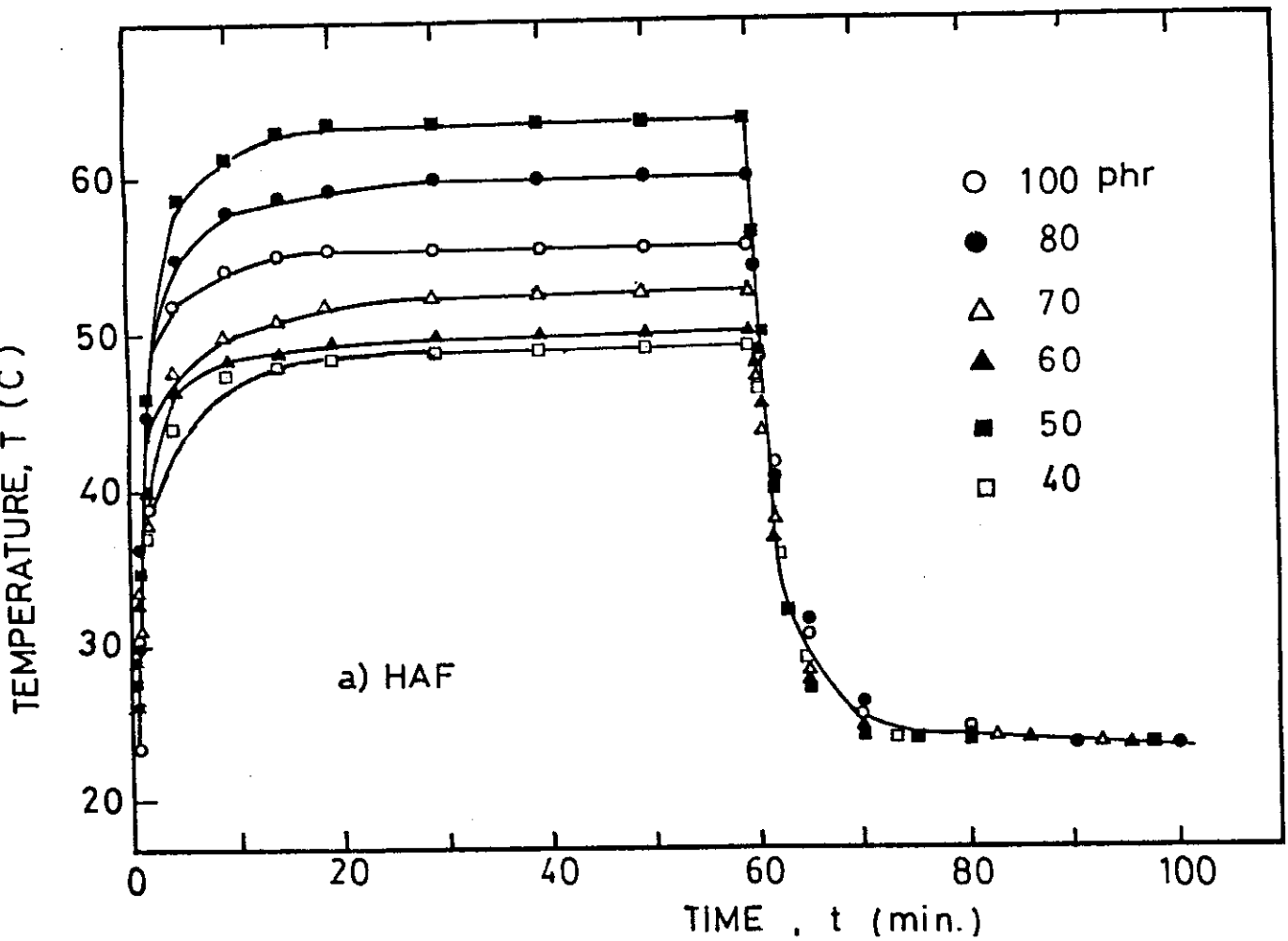

Fig.[4.16]: The temperature-time characteristics for HAF black-loaded butyl rubber vulcanizates.

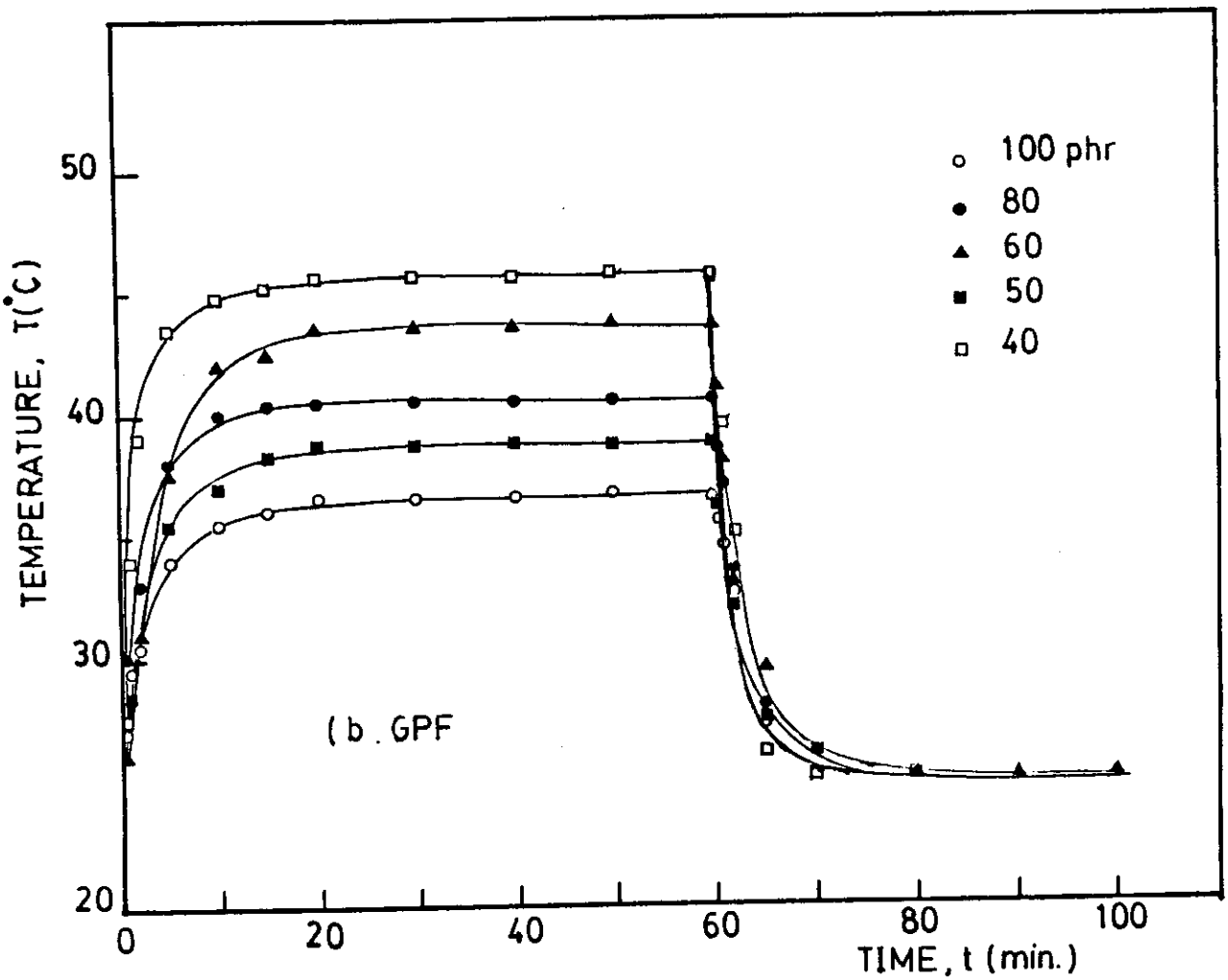

Fig.[4.17]: The temperature-time characteristics for GPF black-loaded butyl rubber vulcanizates.

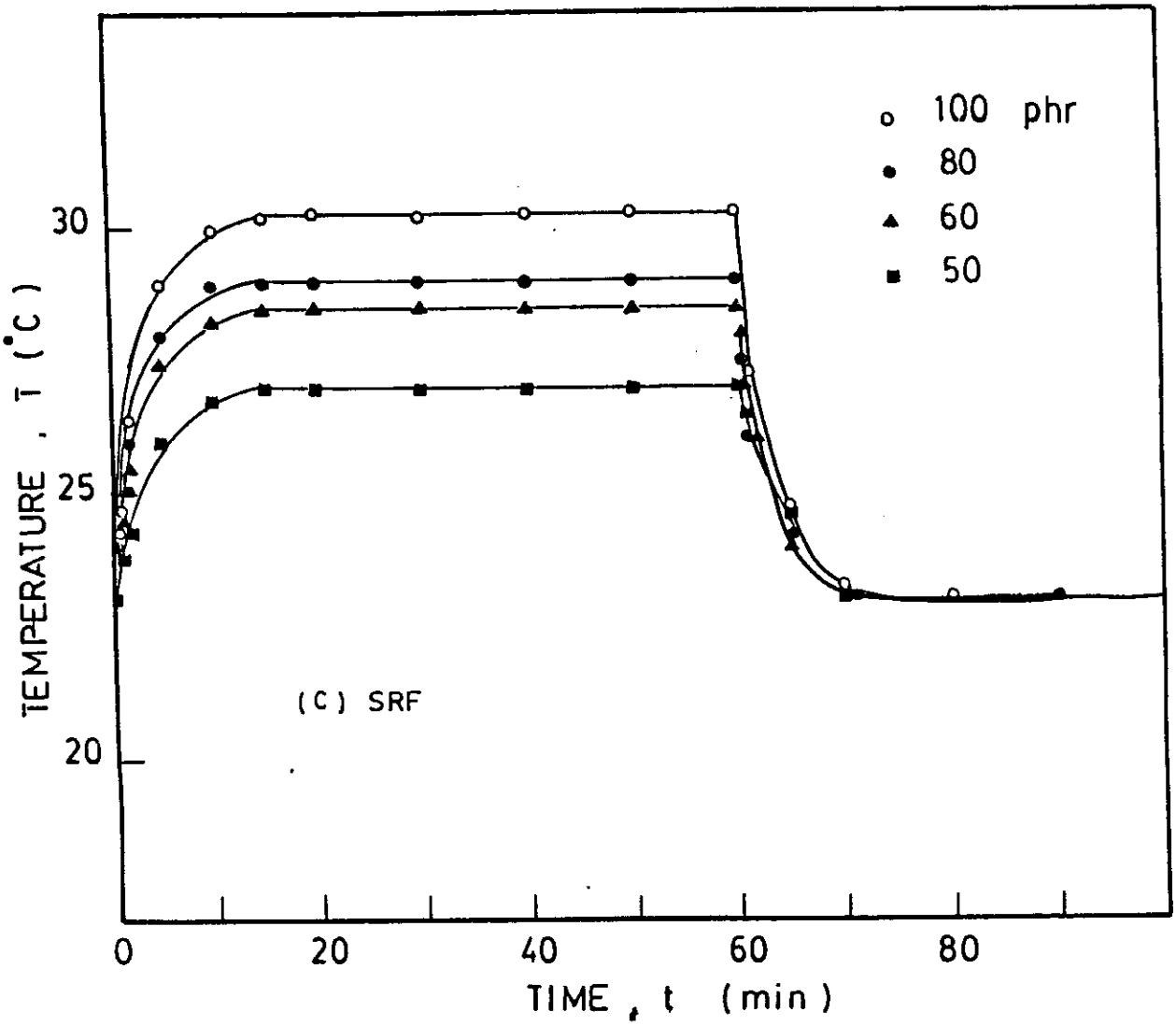

Fig. [4.18] : The temperature-time characteristics for SRF black-loaded butyl rubber vulcanizates.

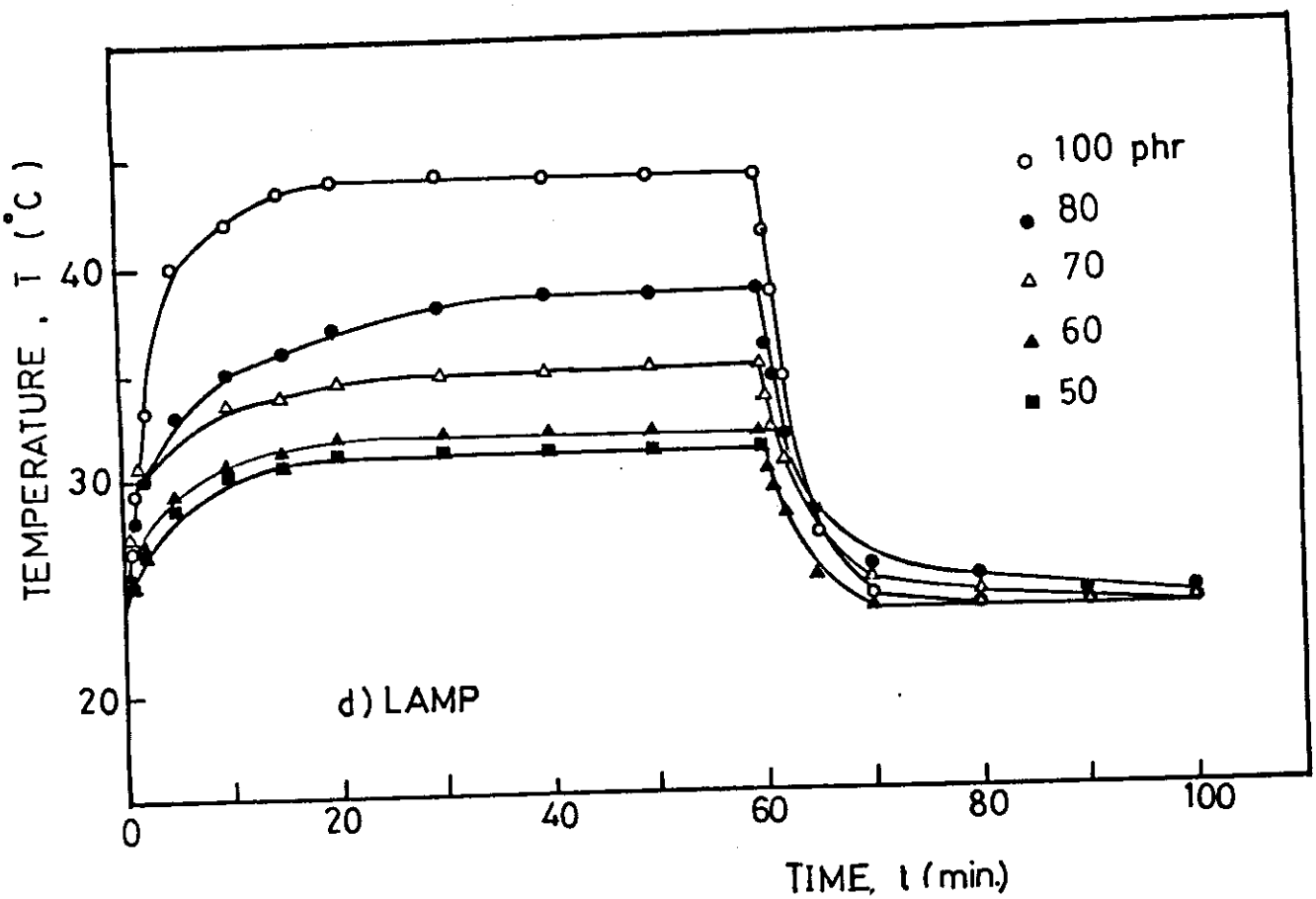

Fig.[4.19]: The temperature-time characteristics for LAMP black-loaded butyl rubber vulcanizates.

Table. 4.7 : The calculated values of the time constants τ_g, τ_i, and τ_d, specific heat and the amount of heat transferred by radiation and convection.

Sample	τ_g (min)	τ_i (min)	τ_d (min)	C_{p_I} [J/gm.deg]	$C_{p_{III}}$ [J/gm.deg]	$(h_r + h_c)$ [J/m^2 deg.sec]
CH10	2.17	0.67	2.70	3.95	2.75	36.4
CH8	2.50	0.27	3.85	3.21	4.70	34.0
CH7	2.67	0.14	2.78	3.88	4.16	45.0
CH6	2.60	0.29	2.86	4.42	4.94	44.4
CH5	2.33	0.16	2.10	2.13	3.19	43.4
CH4	2.25	0.20	2.90	4.10	5.80	47.5
CG10	3.33	0.37	3.85	4.17	5.18	55.6
CG8	2.70	0.37	3.70	3.46	4.80	42.8
CG6	4.55	0.15	3.57	3.36	3.75	37.0
CG5	3.47	0.11	2.94	2.43	3.75	43.0
CG4	2.20	0.13	1.60	1.54	1.71	28.2
CS10	2.70	0.27	2.70	3.14	3.37	44.1
CS8	2.63	0.23	3.23	3.00	4.00	46.0
CS6	2.90	0.40	2.86	3.51	3.83	46.5
CS5	4.55	0.16	5.00	4.17	4.24	55.0
CL10	3.00	0.14	2.85	3.25	2.65	28.4
CL8	5.00	0.04	4.40	2.88	3.64	22.8
CL7	3.10	0.23	4.40	3.32	3.87	24.2
CL6	4.65	0.08	3.00	2.95	4.41	42.0
CL5	5.00	0.10	3.33	3.72	3.64	32.0

specific heat [C_{p_I} and $C_{p_{III}}$] for different types and concentrations of carbon black as well as the time constants [τ_i, τ_g, and τ_d]. The average specific heat [[C_{p_I} + $C_{p_{III}}$] / 2] were plotted against the carbon black concentration, as shown in figure 4.20

It is clear from this figure that as the carbon black concentration increases the specific heat of their corresponding composites decreases. This decrease in the specific heat with increasing carbon black concentration may be attributed to the fact that specific heat of rubber [≅ 1.7 Joule/gm.deg.][3] is higher than that of carbon black [≅ 1.25 Joule/ gm.deg.][3].

The heat produced, by Joule effect, per watt is plotted as a function of carbon black concentration. Figure 4.21 represents the dependence of ΔT/P on the concentration for the different types of carbon black. From this figure it may be concluded that there is a certain concentration for every type of carbon black at which maximum value of ΔT/P is obtained.

Table 4.8 shows the calculated values of the thermal conductivity, λ, thermal diffusivity, δ, and specific heat, Cp for different types and concentrations of carbon black-loaded

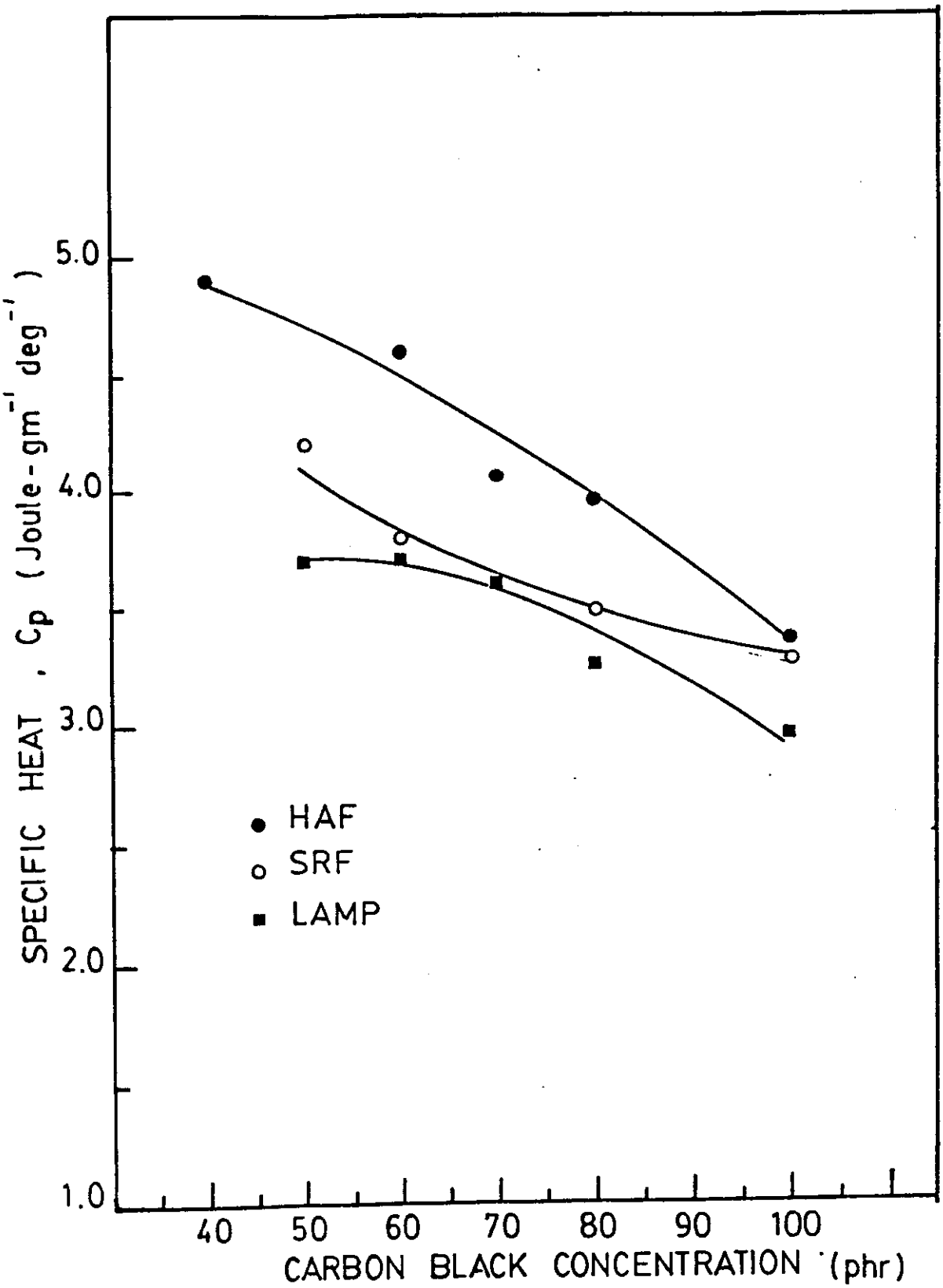

Fig. [4.20] : The dependence of the specific heat on carbon black concentrations.

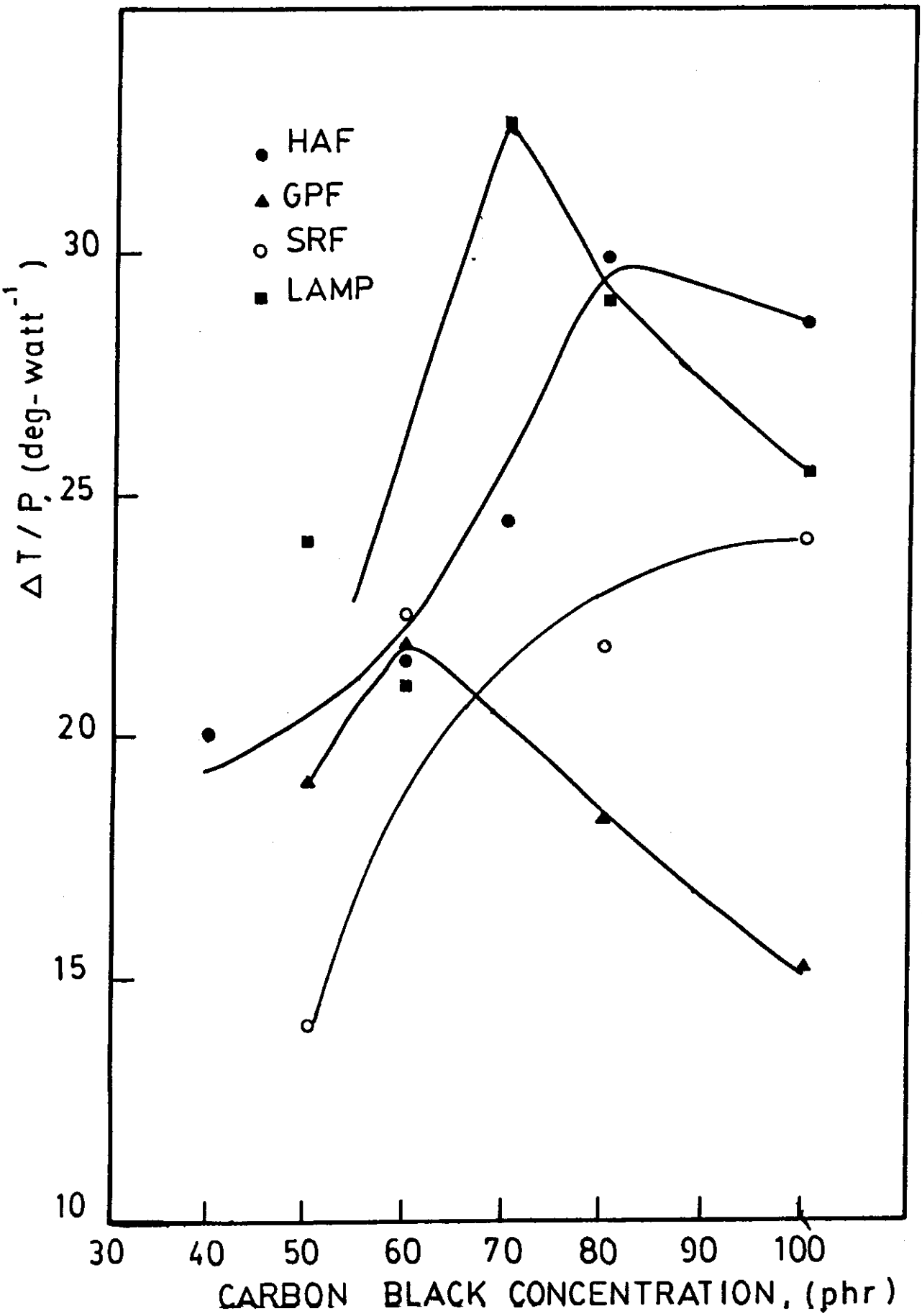

Fig. [4.21] : The dependence of ΔT/P on the carbon black concentrations.

Table 4.8 : The calculated values of the thermal conductivity λ, thermal diffusivity and specific heat C_p for the investigated rubber composites.

Sample	λ [Watt/m deg.]	δ [cm^2/sec.]	C_p [J/gm.deg.]
CH10	0.725	1.3×10^{-3}	4.00
CH8	0.313	1.2×10^{-3}	2.00
CH7	0.310	1.2×10^{-3}	2.00
CH6	0.604	1.4×10^{-3}	3.40
CH5	0.385	1.1×10^{-3}	2.83
CH4	0.617	8.8×10^{-4}	5.70
CG10	0.437	1.1×10^{-3}	2.32
CG8	0.457	1.1×10^{-3}	3.00
CG6	0.318	1.0×10^{-3}	2.50
CG5	0.564	1.1×10^{-3}	4.12
CG4	0.399	1.0×10^{-3}	3.24
CS10	0.728	1.4×10^{-3}	3.93
CS8	0.438	1.4×10^{-3}	2.41
CS6	0.370	9.7×10^{-4}	3.00
CS5	0.780	1.2×10^{-3}	5.23
CS4	0.366	9.3×10^{-4}	3.26
CL10	0.540	1.5×10^{-3}	2.73
CL8	0.313	1.6×10^{-3}	1.50
CL7	0.380	1.2×10^{-3}	2.32
CL6	0.416	1.2×10^{-3}	2.82
CL5	0.608	8.1×10^{-4}	6.00
CL4	0.528	1.1×10^{-3}	3.92

butyl rubber composites. Its noticed from this table that, the comparison of the data for the specific heat, C_p calculated by the flash method [Tables 4.6 and 4.8] are in a good agreement with that calculated before [Cf. Tables 4.5 and 4.7].

4.4 : Other Factors Affecting the Electrical and Thermal Effects of Carbon Black-Loaded Butyl Rubber :

For obtaining the optimum conditions required for these heating elements *some factors* affecting the electrical and thermal parameters of conductive butyl rubber composites were studied. These factors are the ambient temperature, the sample dimensions. Measurements using the alternating current as convential power main. and ageing of the samples under *continuous* electric power application, up to 6 months were made.

4.4.1 : Effect of the Ambient Temperature :

In order to show the effect of the ambient temperatures, on the thermal performance of the rubber heating elements, the T-t characteristic curves for composites containing 100 phr carbon black/[IIR + 20 phr $BaTiO_3$] at different ambient temperatures were obtained.

The ambient temperature was controlled by using an ultrathermostate in the range from 0 to 70°C .

Figure 4.22 illustrates the the difference in temperature-

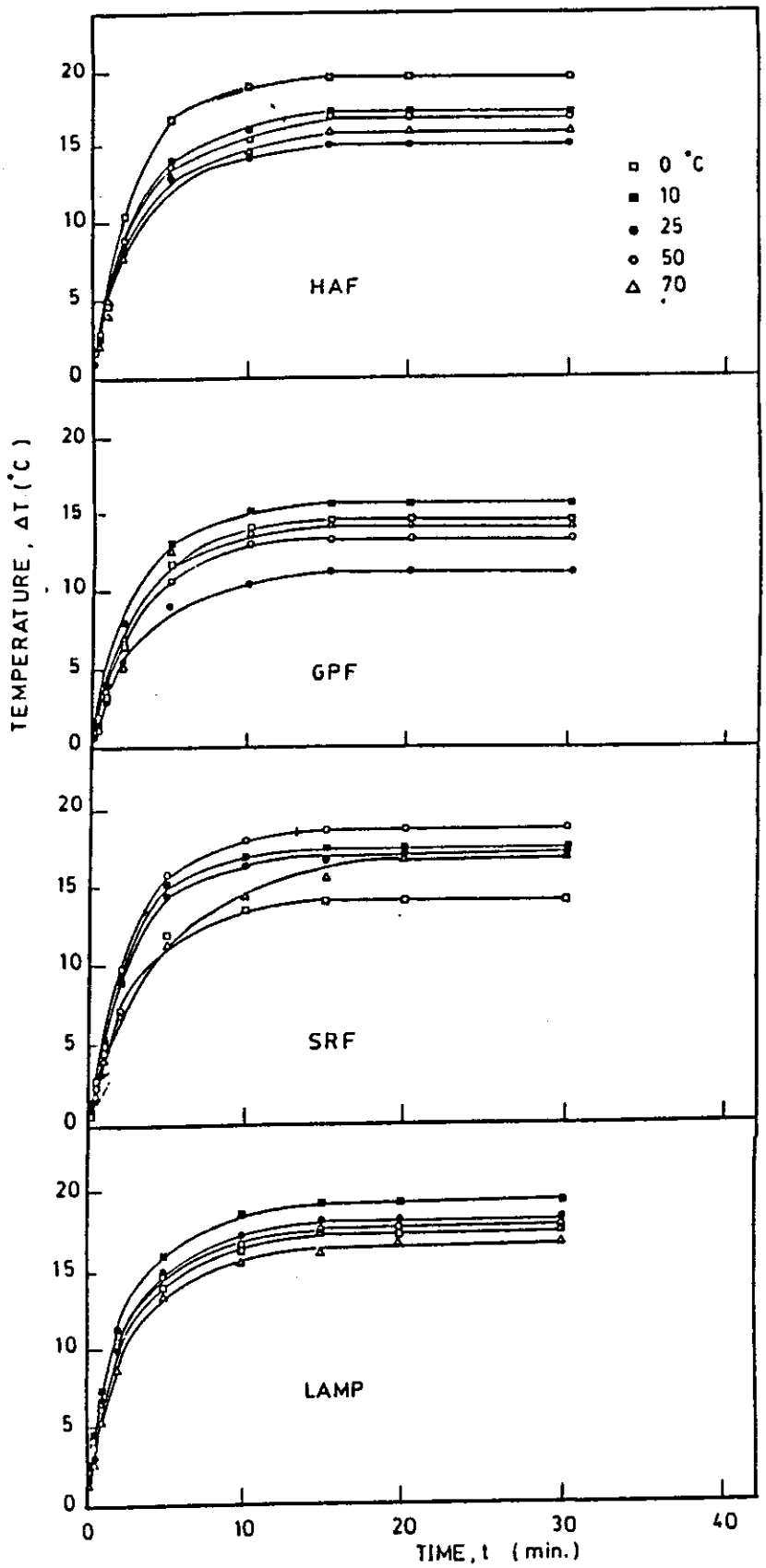

Fig. [4.22] : ΔT-t characteristics for the different types of carbon black at different ambient temperatures.

time [ΔT-t] characteristic curves for the different types of carbon black at different ambient temperature . From this figure it is clear that the variation in the ambient temperature markedly affects the difference in temperature [ΔT] produced by Joule heating. Figure 4.23 summerizes the dependence of the ultimate temperature difference on the ambient temperature. It is obvious from this figure that a maximum value of ΔT was produced, in general, at ambient temperature of 10°C.
In other words the quantity of heat transfer per unit area per degree has its maximum value at ambient temperature equal 10°C.

These results were confirmed by the measurements of the specific heat, C_p, at different ambient temperatures, [figure 4.24]. In this case the minimum value observed in the specific heat is attained at 10°C for all types of conductive rubber composites.

4.4.2 : Effect of the Sample Dimensions :

In this subsection the effect of the dimensions of the

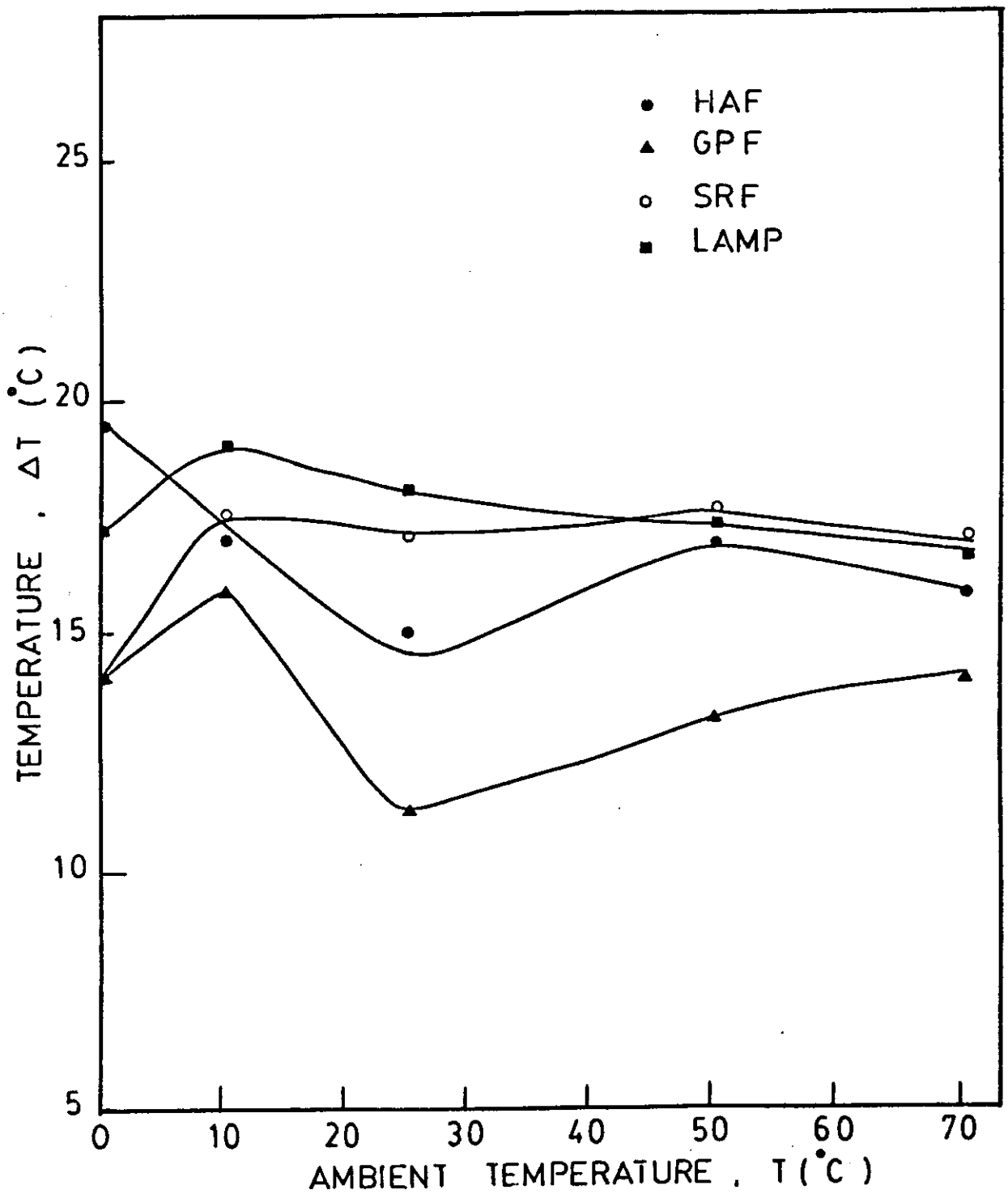

Fig. [4.23] : The dependence of the temperature difference, ΔT on the ambient temperature at initial power = 1 watt.

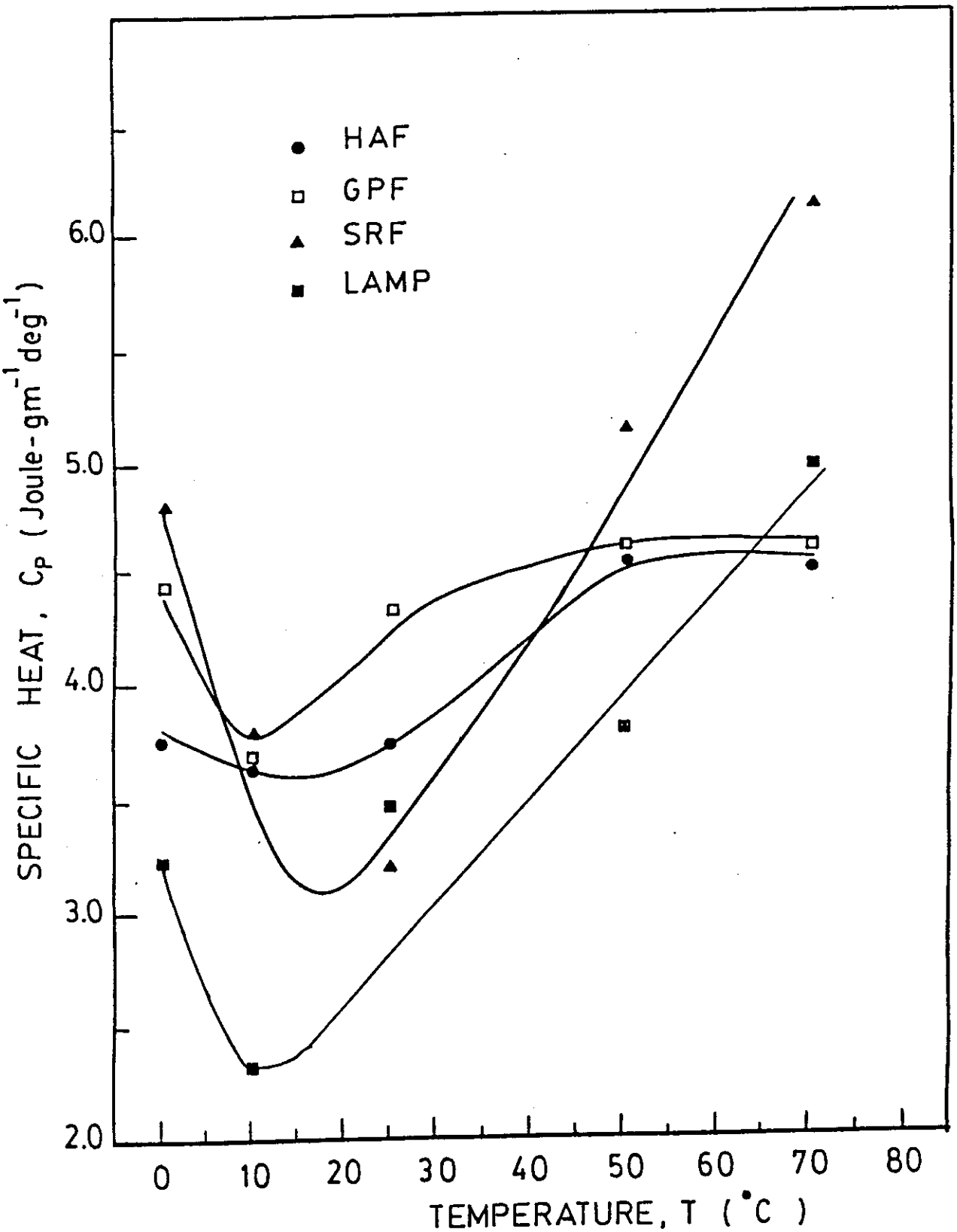

Fig. [4.24] : The specific heat dependence on the ambient temperature.

electric heater on its thermal parameters was studied. For this purpose, different test samples having different dimensions and containing [100 phr HAF/[IIR + 20 $BaTiO_3$]] were used.

Figure 4.25 illustrates the dependence of the temperature difference per watt on S/V, where S is the sample surface area, cm^2, and V its volume, cm^3. From this figure it is clear that the difference in temperature, ΔT, produced by Joule heating effect, increases as S/V increases.

In a trial to correlate the total heat capacity [$M C_p$] of the rubber composite with the heat capacities of its ingredients , the following rule of additivity was used :

$$M C_p = m_1 C_{p1} + m_2 C_{p2} + \ldots\ldots + m_n C_{pn} \qquad (4.13)$$

where $M C_p$ is the heat capacity of the composite, and $m_1 C_{p1}$, $m_2 C_{p1}$, ..., $m_n C_{pn}$ are the heat capacities of the ingredients.

Figure 4.26 shows the relation between the heat capacity and the sample mass. The solid curve represents the values of

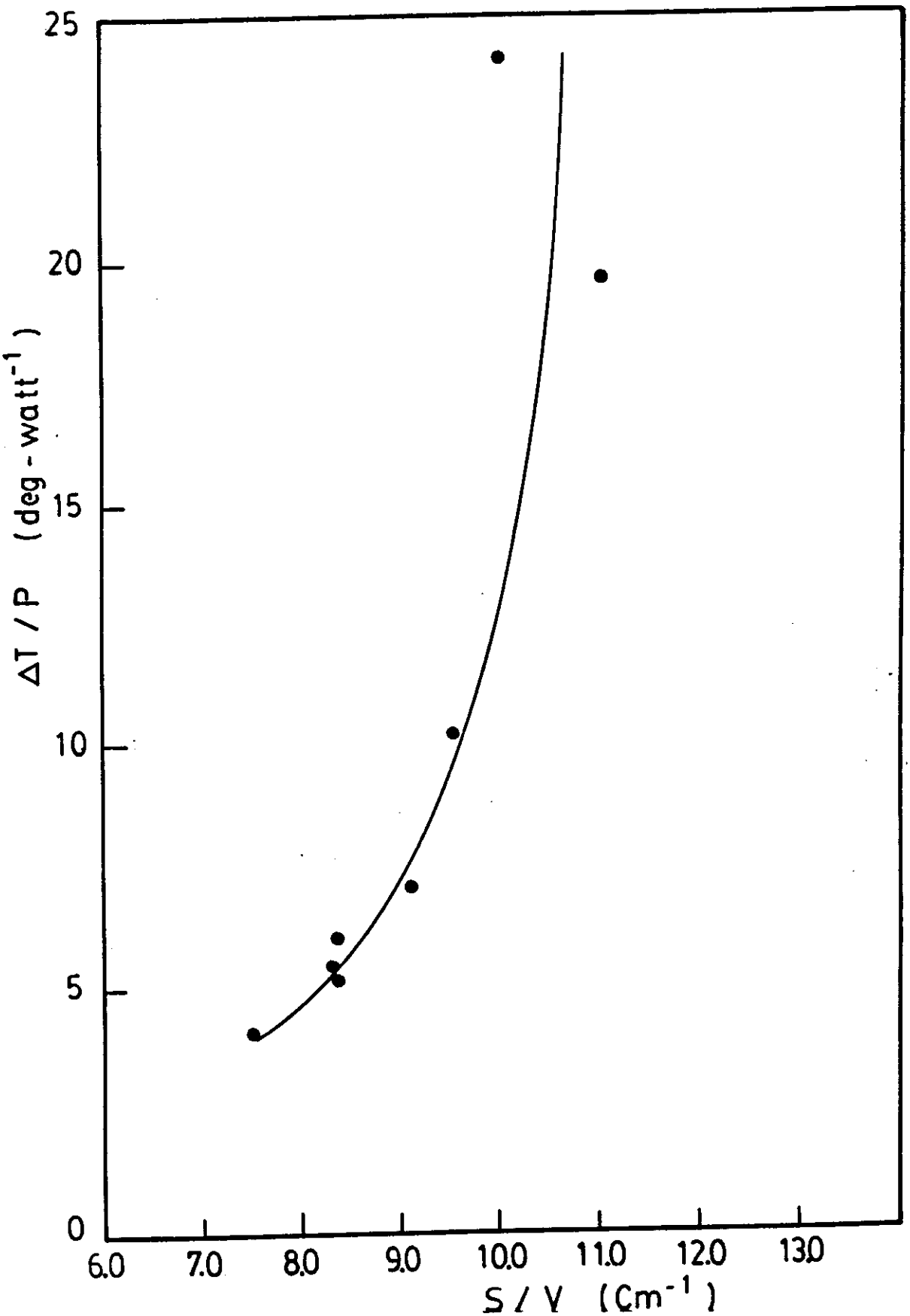

Fig. [4.25]: The dependence of the temperature difference per watt on Surface to Volume [S/V] ratio of the investigated 100 phr HAF/(IIR + 20 phr $BaTiO_3$) rubber sample.

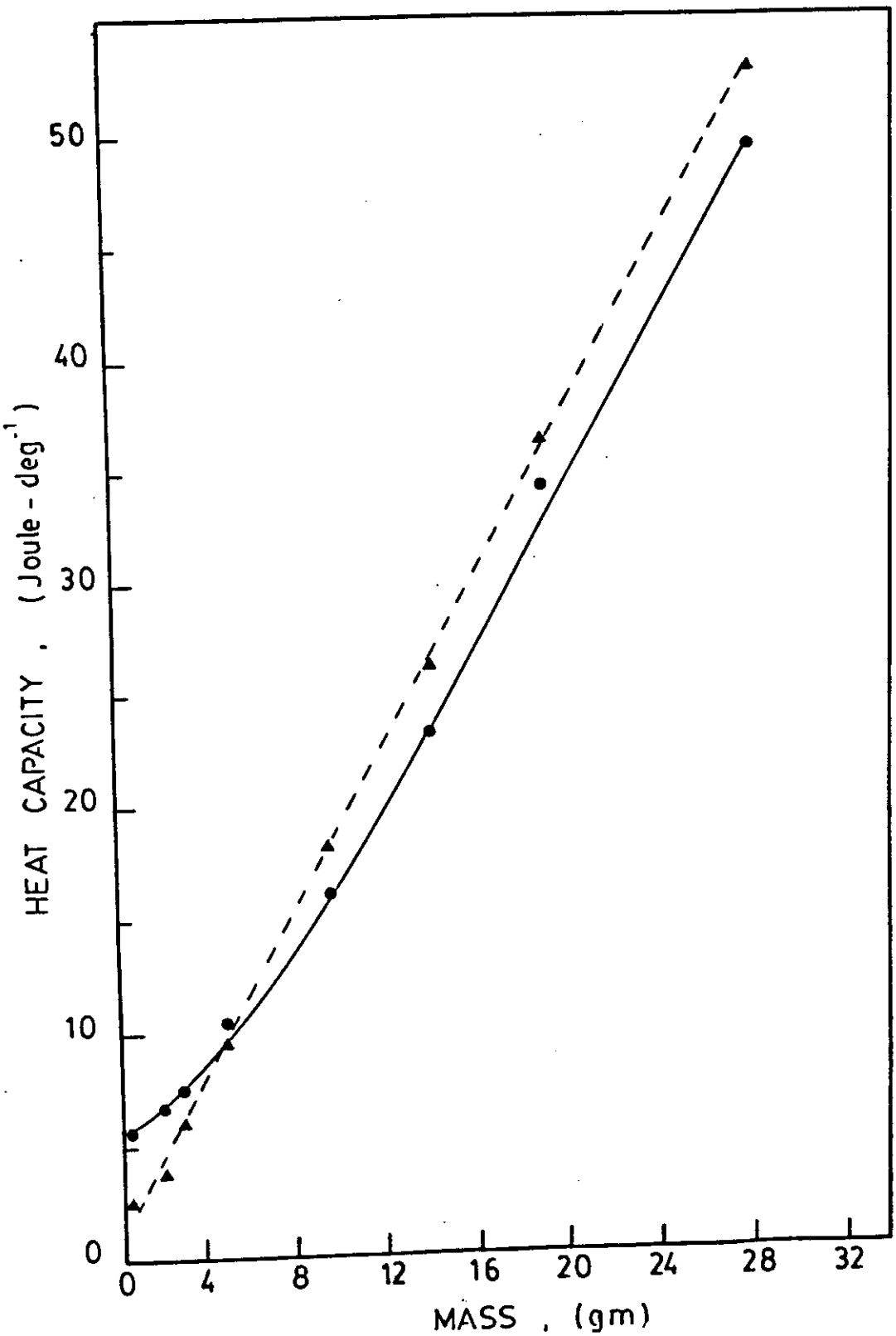

Fig. [4.26] : The dependence of the heat capacity on the mass of the investigated rubber composite. The solid line represents the calculated values of MC_p and the dashed one is the values obtained by the rule of additivty.

the heat capacities which are produced by multiply every mass of the composite by its calculated specific heat, and the dashed line represents the values of the heat capacities which are produced by the summations of the heat capacities for every ingredient, [rule of additivity, eqn 4.13].
From this figure it is clear that the two values of the heat capacities, which produced experimentally and by using the rule of additivity, for any mass are practically the same.
Thus, by knowing the heat capacity of each ingredient and its concentration , one can predict the heat content of the corresponding composites.

4.4.3 : AC - Measurements :

The study in this subsection was extented to carry out our measurements by using ac [50 Hz.] as a power supply. The samples containing 100 phr of carbon black with 20 phr $BaTiO_3$ were used in this study. They were subjected to the electrical and thermal measurments as shown in figure 4.27 which illustrates the current - voltage - temperature [I - V - T] characteristics as well as the temperature-

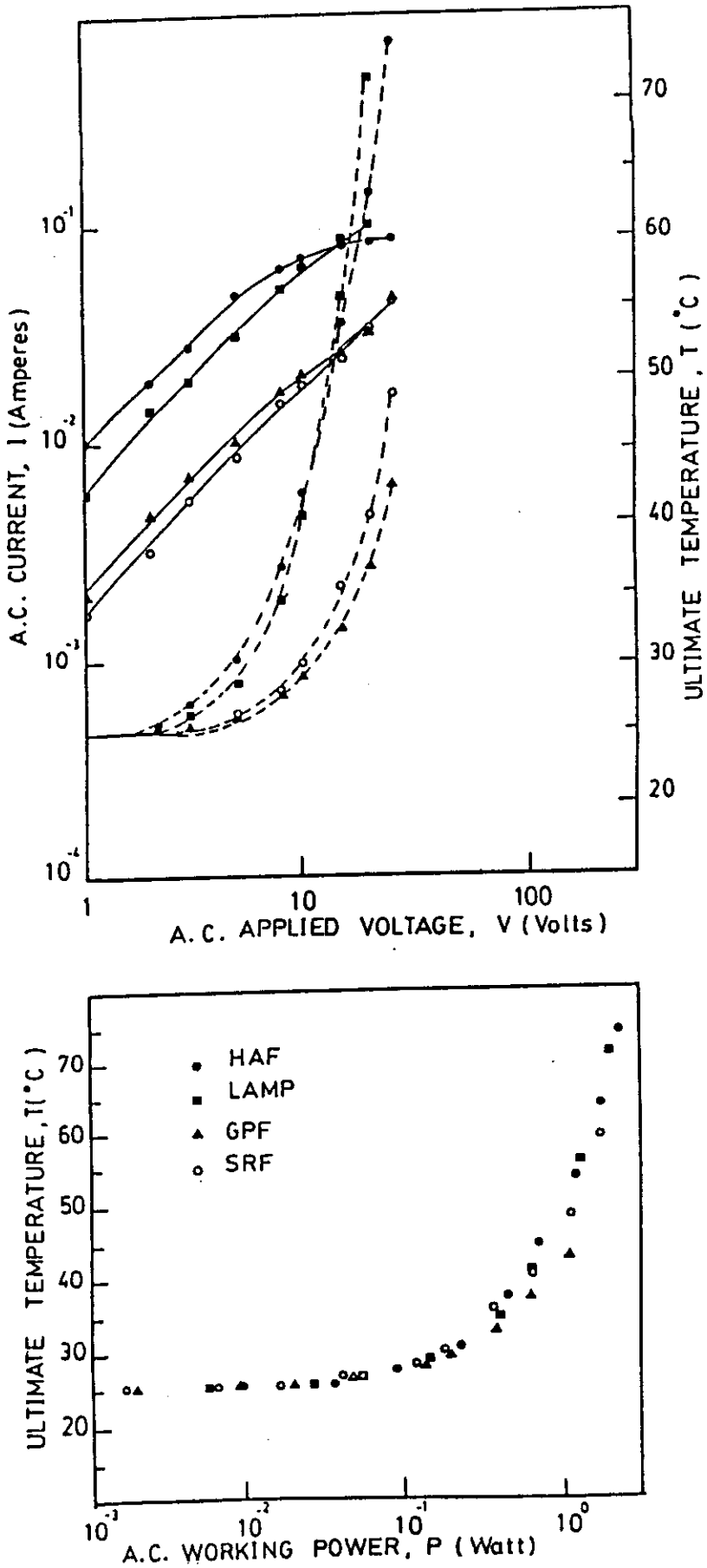

Fig. [4.27] : I-V-T and T-P curves for carbon black-loaded butyl rubber composites. *[alternating current].*

power [T-P] curves. If a comparison was made between this data and that of the dc-measurments, shown before [figures 4.4 and 4.6.b], one can conclude that, the samples containing SRF and LAMP blacks, possess higher ΔT in case of dc-supply than ac-supply at the same applied electric power. Table 4.9 illustrates the values of the fitting parameters a and b, from equation 4.2. From this Table it is clear that, for composites containing SRF and LAMP blacks, the values of a, [ΔT at P = 1 watt], is higher in case of dc-supply than these in case of ac-supply. On the other hand these values of ΔT remain the same for samples containing HAF and GPF blacks independent of the type of power supply.

4.4.4 : Ageing of Samples :

In order to study the effect of ageing on the electrical and thermal performance of the rubber heating elements, the above conductive sampls were subjected to ac - electric power for different time intervals.

The ambient temperature was fixed at 10°C by using an incubator. The I - V - T characteristic curves were taken

Table. 4.9 : The calculated values of the fitting parameters a and b [from equation **4.1**] in case of dc and ac-power supply.

Sample	D C		A C	
	a (deg)	b	a (deg)	b
CH10	26.0	1.14	25.4	0.96
CG10	18.0	0.85	18.0	0.96
CS10	31.6	1.00	23.0	0.91
CL10	25.5	0.97	22.0	0.95

every week with a continuous application of the heating power.

Figures 4.28 - 4.31 illustrate the current - voltage - temperature characteristic curves for different periods of the working time for the four types of carbon black ; a) HAF, b) GPF, c) SRF, and d) LAMP black. It is clear from these figures that no appreciable changes in the electrical and the thermal measurments were detected after periodes of working time *exceeding 6 months* for HAF, GPF, and SRF blacks, while for LAMP black the sample current *decreases* after 3 months and consequently, the heat produced by Joule effect was reduced.

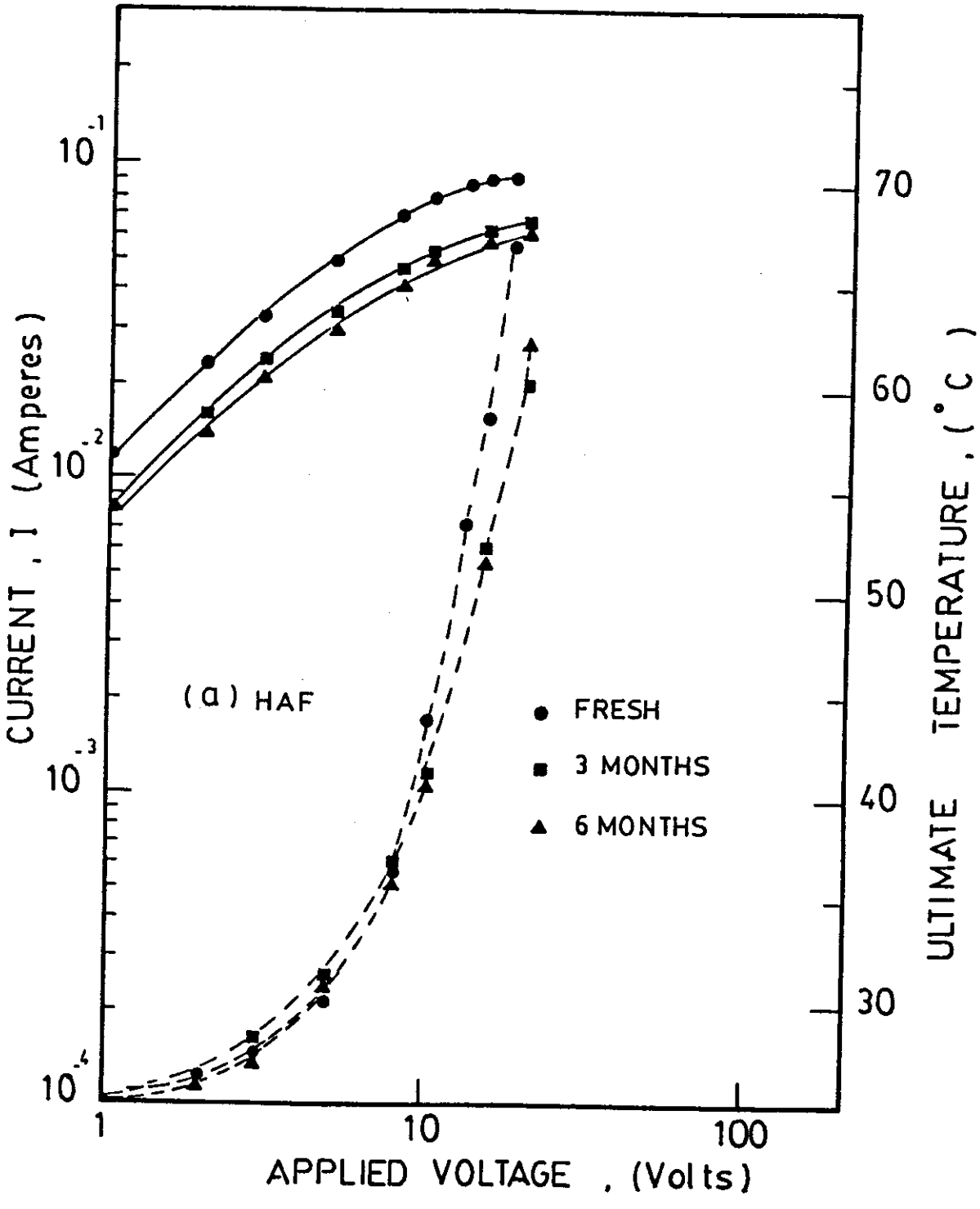

Fig. [4.28] : I-V-T curves for different periods of working time for 100 phr HAF/[IIR+20 phr BaTiO3] rubber composite.

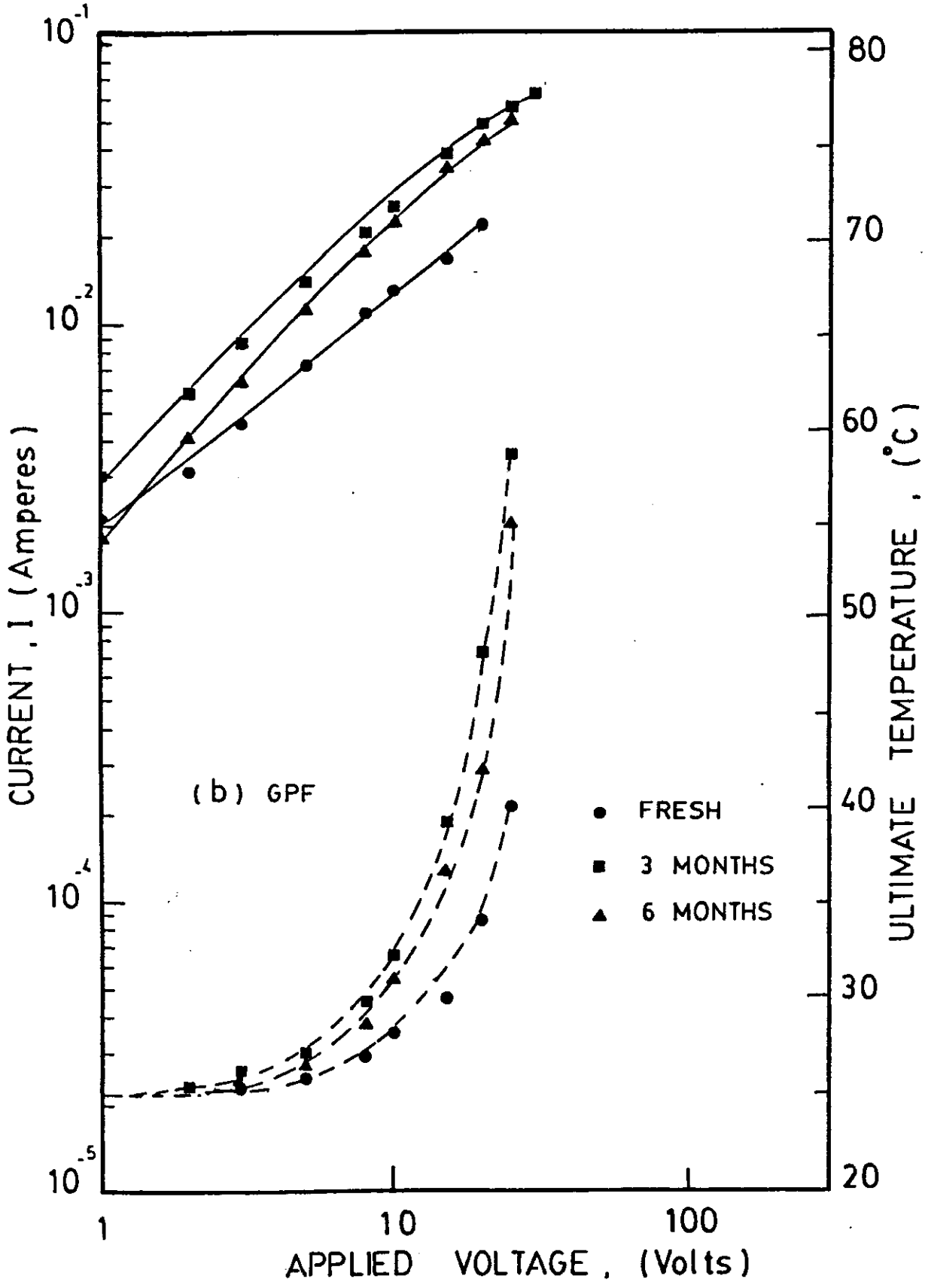

Fig. [4.29] : I-V-T curves for different periods of working time for 100 phr GPF/[IIR+20 phr $BaTiO_3$] rubber composite.

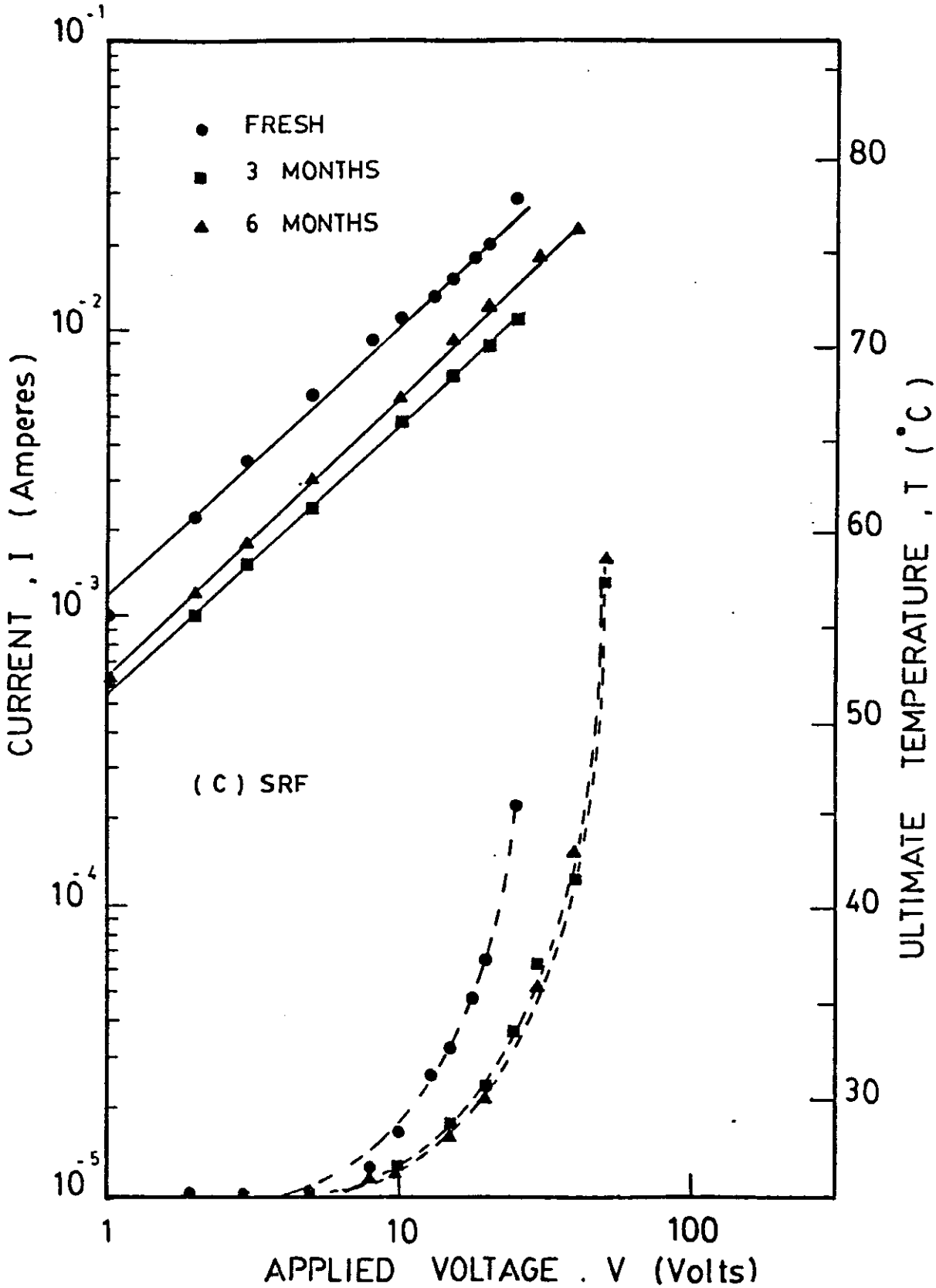

Fig. [4.30] : I-V-T curves for different periods of working time for 100 phr SRF/[IIR+20 phr $BaTiO_3$] rubber composite.

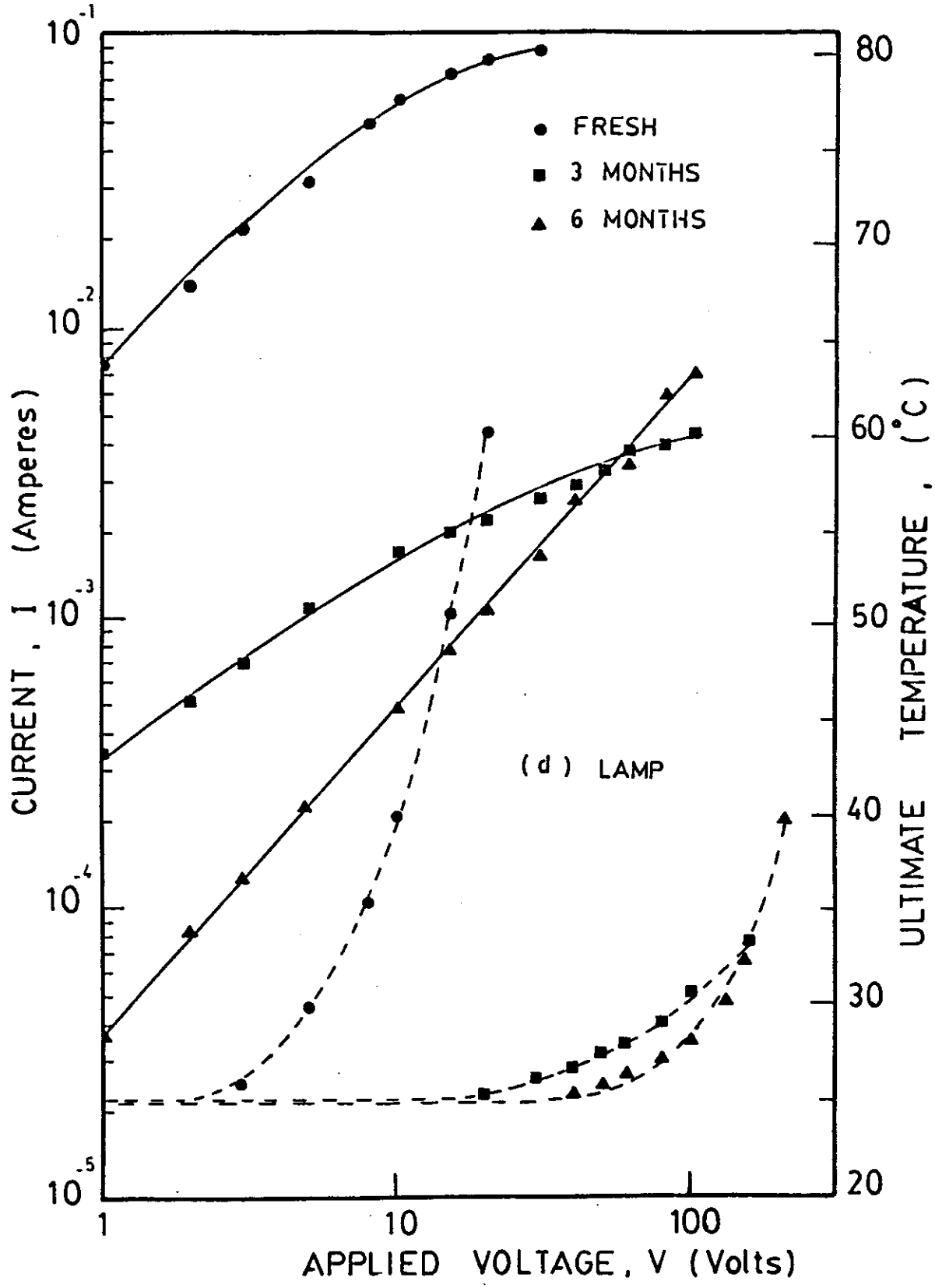

Fig. [4.31] : I-V-T curves for different periods of working time for 100 phr LAMP/[IIR+20 phr $BaTiO_3$] rubber composite.